ERDC/GSL TR-21-16

US Army Corps
of Engineers®
Engineer Research and
Development Center

ERDC
ENGINEER RESEARCH & DEVELOPMENT CENTER

Alternatives for Large Crater Repairs using Rapid Set Concrete Mix®

Lulu Edwards, Haley P. Bell, and Marcus L. Opperman

June 2021

Geotechnical and Structures Laboratory

The U.S. Army Engineer Research and Development Center (ERDC) solves the nation's toughest engineering and environmental challenges. ERDC develops innovative solutions in civil and military engineering, geospatial sciences, water resources, and environmental sciences for the Army, the Department of Defense, civilian agencies, and our nation's public good. Find out more at www.erdc.usace.army.mil.

To search for other technical reports published by ERDC, visit the ERDC online library at https://erdclibrary.on.worldcat.org/discovery.

ERDC/GSL TR-21-16
June 2021

Alternatives for Large Crater Repairs using Rapid Set Concrete Mix®

Lulu Edwards, Haley P. Bell, and Marcus L. Opperman

Geotechnical and Structures Laboratory
U.S. Army Engineer Research and Development Center
3909 Halls Ferry Road
Vicksburg, MS 39180-6199

Final report

Prepared for Headquarters, U.S. Air Force Civil Engineer Center
Tyndall Air Force Base, FL 32403-5319

Under MIPR F4ATA78038GW01

Abstract

Research was conducted at the U.S. Army Engineer Research and Development Center (ERDC) in Vicksburg, MS, to identify alternative repair methods and materials for large crater repairs using Rapid Set Concrete Mix®. This report presents the technical evaluation of the field performance of full-depth slab replacement methods conducted using Rapid Set Concrete Mix® over varying strength foundations. The performance of each large crater repair was determined by using a load cart representing one-half of the full gear of a C-17 aircraft. Results indicate that using rapid-setting concrete is a viable material for large crater repairs, and the performance is dependent on surface thickness and base strength.

Contents

Figures and Tables

Figures

Tables

Preface

This study was conducted for the U.S. Air Force Civil Engineer Center (AFCEC) under the Rapid Airfield Damage Recovery (RADR) program, MIPR F4ATA78038GW01. The research was performed by the Airfields and Pavements Branch (GMA) of the Engineering Systems and Materials Division (GM), U.S. Army Engineer Research and Development Center, Geotechnical and Structures Laboratory (ERDC-GSL). The Program Manager was Mr. Jeb S. Tingle, ERDC-GSL. The technical monitor was Dr. Robert Diltz, AFCEC.

At the time of publication, Ms. Anna M. Jordan was Chief, GMA; Mr. Justin S. Strickler was Chief, GM; and Mr. R. Nicholas Boone, GVT, was the Technical Director for Force Projection and Maneuver Support. Mr. Charles W. Ertle II was Deputy Director of ERDC-GSL, and the Director was Mr. Bartley P. Durst.

COL Teresa A. Schlosser was the Commander of ERDC, and Dr. David W. Pittman was the Director.

1 Introduction

1.1 Background

The purpose of the Rapid Airfield Damage Recovery (RADR) program is to develop capabilities to rapidly repair damaged airfields for the full spectrum of operational scenarios. The operational scenarios include base recovery after an attack, expedient repairs at deployed locations, and sustainment of operating surfaces at forward operating bases. Cementitious, rapid-setting concrete repair materials have been successfully used as a capping material for repairing bomb-damaged airfield concrete pavements under the RADR program. Since 2006, over 200 repairs have been conducted using proprietary, rapid-setting concrete repair materials. Data collected throughout numerous field trials during this time indicated that the use of several different commercial products can produce a repair that withstands aircraft traffic following a short curing time of 2 hr. Based on results from the numerous field projects, Rapid Set Concrete Mix® was identified as a versatile repair material and was recommended for a variety of repair types including spall repair, small and large patches, full-slab replacements, and small and large crater repairs (Priddy 2011; Priddy et al. 2016).

Successful field results under simulated and actual C-17 and F-15E aircraft maneuvers (Priddy et al. 2011), ease-of-placement, and versatility with concrete mixing equipment led to the recommendation of Rapid Set Concrete Mix® repair material for RADR operational scenarios with potential application to peacetime repair activities. These peacetime repair activities include any repairs not associated with bomb damage such as spall repairs, partial slab replacements, and full slab replacements caused by overloading of the pavement by aircraft or loss of foundation support. While numerous repairs have been conducted with rapid-setting concrete materials, specific guidance is lacking on the number of aircraft passes Rapid Set Concrete Mix® can sustain when used as a repair material for large craters. Large craters are defined as craters with diameters of 15 ft or more.

1.2 Objective

The objective of the research presented in this report was to assess the operational effectiveness and suitability of methods to repair large

craters. A secondary objective was to identify necessary adjustments to the materials, equipment, and procedures as set in the U.S. Air Force's 2019 Techniques, Tactics, and Procedures (TTP). The goal of this project was to develop large crater repair alternatives capable of sustaining a target of 3,500 C-17 aircraft passes (2,991 coverages) and a target of at least 500 C-17 aircraft passes (427 coverages).

A combination of 14 in. of flowable fill backfill and 10 in. of a rapid-setting concrete surface is currently recommended in the TTP for craters less than 15 ft to achieve 3,000 aircraft passes. For large crater repairs, the TTP recommends the same combination of 14 in. of flowable fill backfill with a 10-in.-thick rapid-setting cap, but crushed stone is another backfill alternative if flowable fill is unavailable.

1.3 Scope

To achieve the project objective, seven large crater repair tests were completed on two full-scale portland cement concrete (PCC) test sections at the U.S. Army Engineer Research and Development Center's (ERDC's) Outdoor Pavement Test Facility in Vicksburg, MS. The repair sizes were either 25 ft by 30 ft or 30 ft by 30 ft. CTS Rapid Set Concrete Mix® was used as the surface material for all seven repairs. Crushed limestone, rapid-setting flowable fill, and cement-stabilized silty sand were used as backfill materials. The compacted subgrade material for all repairs consisted of a low-plasticity lean clay.

Upon completion of each large crater repair, simulated aircraft traffic using a C-17 load cart was applied until failure of the repair or up to 3,500 passes (2,991 coverages). Pavement surface distress data were collected at various trafficking intervals. Forensics, including core-sample extractions for laboratory strength tests, foundation-material strength tests, and surveying data, were conducted after trafficking was completed.

This report describes the full-scale field testing in Chapter 2. Chapter 3 shares details about the pavement structure materials. Chapter 4 presents the repair performance results, while Chapter 5 notes pertinent conclusions and recommendations. The Appendix presents the observations of each repair noted during trafficking.

2 Full-Scale Field Testing

Seven repairs were completed to determine the effects that varying surface thickness, base thickness, and base strength have on repair performance in terms of the passes-to-failure for large crater repairs using rapid-setting concrete. The design matrix for this study is shown in Table 1 and Figure 1. All repair sizes were either 25 ft by 30 ft or 30 ft by 30 ft, depending upon the test section utilized for the repair. The following sections describe the test sections used to conduct repairs, the repair materials, the trafficking procedures, the failure criteria, and the data collection procedures.

Table 1. Repair design matrix.

Repair No.	Rapid Set Concrete Mix® Cap Thickness (in.)	Base Material	Base Thickness (in.)	Base Target CBR (%)	Subgrade Material
1	10	Rapid-Setting Flowable Fill	14	80-100	Lean Clay
2	10	Crushed Limestone	14	80-100	Lean Clay
3	6	Rapid-Setting Flowable Fill	14	80-100	Lean Clay
4	10	Crushed Limestone	20	50	Lean Clay
5	10	Crushed Limestone	20	80-100	Lean Clay
6	14	Crushed Limestone	16	80-100	Lean Clay
7	10	Cement-Stabilized Silty Sand	14	80-100	Lean Clay

Figure 1. Repair design matrix.

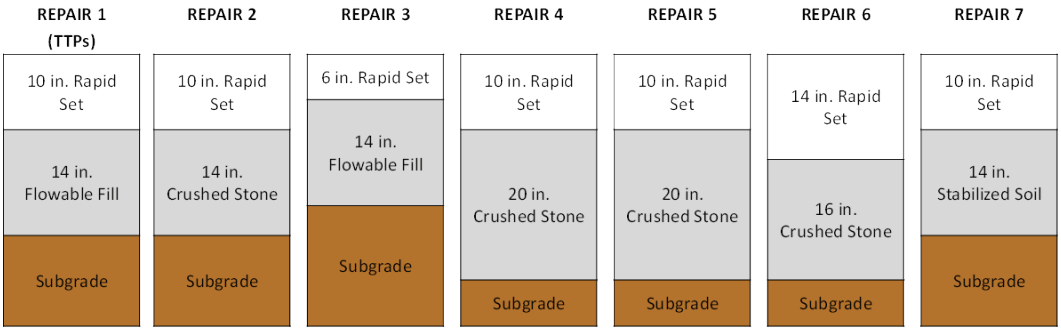

2.1 Test sections

Two existing full-scale concrete test sections located at the ERDC's Outdoor Pavement Test Facility were utilized to conduct the repair tests. Repairs 1 through 4 were completed on a PCC pavement test section constructed in 2011. The original slab sizes consisted of 15-ft by 12.5-ft by 13-in.-thick slabs. The resulting pavement structure consisted of 13 in. of PCC over 6 in. of a crushed gravel base course over 12 in. of a compacted

silty clay subgrade with a soil classification of low-plasticity clay (CL). The average 28-day unconfined compressive strength and flexural strength results on the original test section's concrete were 8,010 and 820 psi, respectively. These average 28-day results are well above the minimum requirements for airfield pavements (5,000 and 650 psi, respectively). Four adjacent slabs and their foundation materials were excavated to create a 25-ft by 30-ft large crater repair area.

Repairs 5 through 7 were completed on a 15-in.-thick PCC pavement test section constructed in 2017. The existing concrete slabs were 15 ft by 15 ft. The pavement structure consisted of 15 in. of PCC over 6 in. of crushed limestone base course and a sand subgrade. The PCC pavement had an average 28-day compressive strength of 6,300 psi. Four adjacent slabs and their foundation materials were excavated to create a 30-ft by 30-ft large crater repair area.

2.2 Repair materials

When pavement repairs are made, the required repair depth depends on the extent of disturbed material. General airfield design and repair guidance (UFC 2001) recommends a minimum repair PCC surface thickness of 6 in. regardless of aircraft type. Other than very shallow repairs requiring only the replacement of a pavement surface, the majority of repairs require the placement of backfill material to provide a base/platform on which to place the cap and to minimize the amount of rapid-setting concrete (or other PCC material) required to complete the repair. The repair materials included in this investigation were Rapid Set Concrete Mix® as the surface capping material placed over backfill consisting of crushed limestone, rapid-setting flowable fill, or cement-stabilized silty sand. Each material is described in the following subsections.

2.2.1 CTS Rapid Set Concrete Mix®

The rapid-setting concrete used for the study was CTS Rapid Set Concrete Mix®. The main cementitious component in the mix is Rapid Set Cement -- a proprietary, calcium sulfoaluminate-based material that accelerates the hardening time. The aggregate used in the mix is 3/8-in. maximum size pea gravel. The dry blend of cementitious material and aggregate is stored in large 3,000-lb super sacks fashioned from woven geotextile fabric and lined with foil to prevent unwanted exposure to moisture. The preblended material requires only the addition of water.

Per manufacturer's recommendation, bulk citric acid can be added to the mix water to increase the working time of the material and to prevent flash setting of material within the mixer at air temperatures greater than 85°F. Aluminum sulfate can be added in bulk to accelerate the set time of the mix for placement of repairs at air temperatures less than 40°F (Edwards et al. 2013). The material can be mixed using a variety of equipment. A simplified volumetric mixer was previously identified as the fastest and most consistent method for mixing and placing rapid-setting concrete (Priddy et al. 2013). The rapid-setting material is placed in a manner similarly to ordinary concrete, but it must be placed expediently since it begins to harden and set within 15 to 30 min.

Unlike ordinary PCC, this material can sustain heavy aircraft traffic within 2 hr after placement. Results collected during several periods of field and laboratory certification testing have shown that this material achieves unconfined compressive strengths (ASTM C39 2020) in excess of 3,000 psi after 2 hr and over 8,000 psi after 28 days. Flexural strengths (ASTM C78 2018a) obtained using this material are in excess of 350 psi after 2 hr and 650 psi after 28 days.

2.2.2 Rapid-setting flowable fill

The rapid-setting flowable fill used for this study was Buzzi Unicem Utility Fill 1-Step 750. This is a rapid-setting flowable fill material that consists of a dry blend of rapid-setting cement and fine aggregates stored in large 3,000-lb super sacks fashioned from woven geotextile fabric and lined with plastic. As with the rapid-setting concrete, the pre-blended material requires only the addition of water to conduct repair activities.

This material was developed specifically for RADR operations because it can be placed expediently without the need of mixing equipment by using the placement technique known as the "dry method" (Priddy et al. 2013). In the "dry method," thin 4- to 6-in.-thick lifts of dry material are placed, and then approximately 40 gal of water is applied to the surface of each lift and allowed to percolate through the dry material.

When used with a rapid-setting concrete pavement surface, the rapid-setting flowable fill provides sufficient bearing capacity for heavy-aircraft pavement applications as demonstrated in numerous field experiments (Bell et al. 2013; Edwards et al. 2013; Priddy et al. 2013; Carruth et al. 2015). The Buzzi-Unicem Utility Fill 1-Step 750 generally provides an unconfined compressive

strength of 250 psi after 30 min of cure time and 750 psi after 3 hr of cure time. Forensic investigations typically reveal a California Bearing Ratio (CBR) of approximately 100% after 24 hr of cure time.

2.2.3 Crushed limestone

A crushed limestone base material, classified by the Unified Soil Classification System (USCS) as poorly graded gravel (GP-GM) with silt and sand (ASTM D2487 2017a), was procured from a local source in Vicksburg, MS (Figure A1). This material was selected for its high compacted strength and availability and from previous experience using this material as a repair backfill material. Previous laboratory tests conducted on this material have shown that the material meets the requirements detailed in UFGS 32.11.16.16: *Base Course for Rigid Paving*.

Figure 2 shows the moisture-density relationship of the crushed stone material. The material was placed and compacted in 3- to 4-in.-thick lifts to prepare a base on which the rapid-setting concrete surface could be placed.

Figure 2. Moisture-density relationship of limestone.

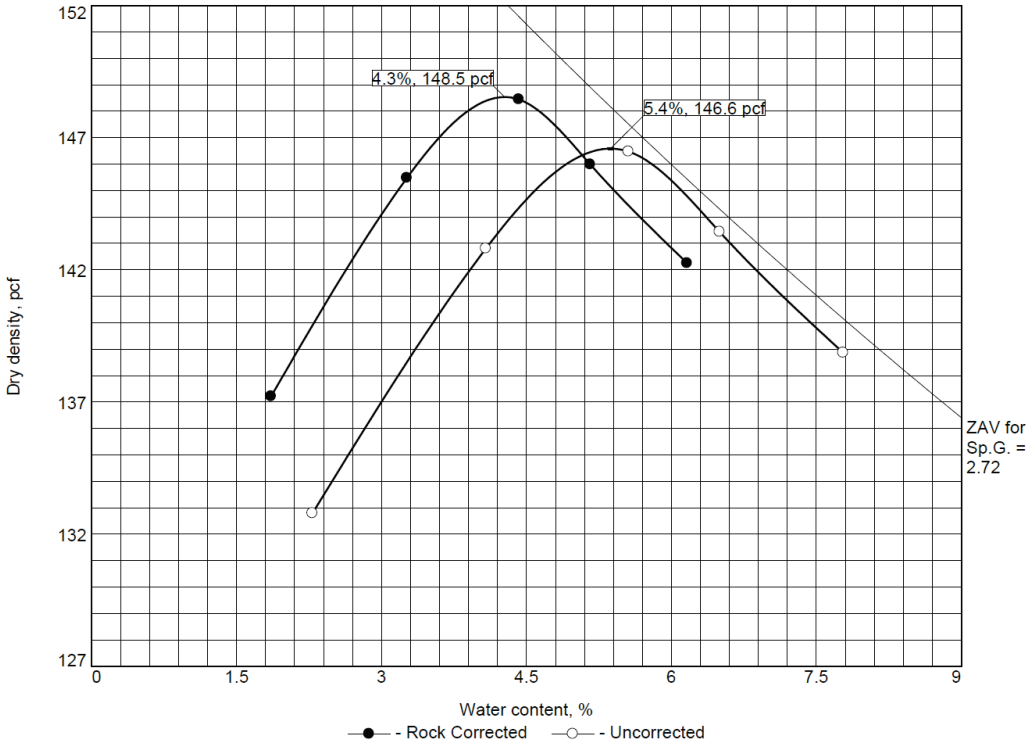

Test specification: ASTM D 1557-12 Method C Modified
ASTM D4718-15 Oversize Corr. Applied to Each Test Point

Elev/ Depth	Classification		Nat. Moist.	Sp.G.	LL	PI	% > 3/4 in.	% < No.200
	USCS	AASHTO						
	GP-GM			2.72			21.6	6.6

ROCK CORRECTED TEST RESULTS	UNCORRECTED	MATERIAL DESCRIPTION
Maximum dry density = 148.5 pcf	146.6 pcf	Gravel (GP-GM) with Silt and Sand, Gray
Optimum moisture = 4.3 %	5.4 %	

2.2.4 Cement-stabilized silty sand

The soil used for the cement-stabilized base course was classified as a silty sand (SM) according to the USCS. Silty sand was selected since it is one of the most abundant naturally available soil types (Robinson and Rabalais 1993). The silty sand blend was created by mixing one part silt to three parts sand. The silty sand was nonplastic (ASTM D4318 2017b) and had the grain-size distribution (ASTM D6913 2017c) shown in Figure A2. The material had a specific gravity of 2.7 (ASTM D854 2014), and the moisture-density relationship (ASTM D1557 2012) is plotted in Figure 3. The soil testing indicated that the maximum density, 128.9 lb/ft^3, occurs at an optimum moisture content of 8.0%.

A Type 1 portland cement was used as a stabilization additive for the silty sand backfill mixture. The portland cement was packaged in 94-lb bags. The silty sand was first spread into a 21-ft by 25-ft by 1-ft-thick section on a flat surface near the crater repair area, and 18 cement bags were placed in a grid pattern on top of the silty sand to evenly disperse the additive to produce a mixture of 5% additive by dry weight. The cement was then mixed with the soil as described in Section 3.3.

Figure 3. Moisture-density relationship of silty sand.

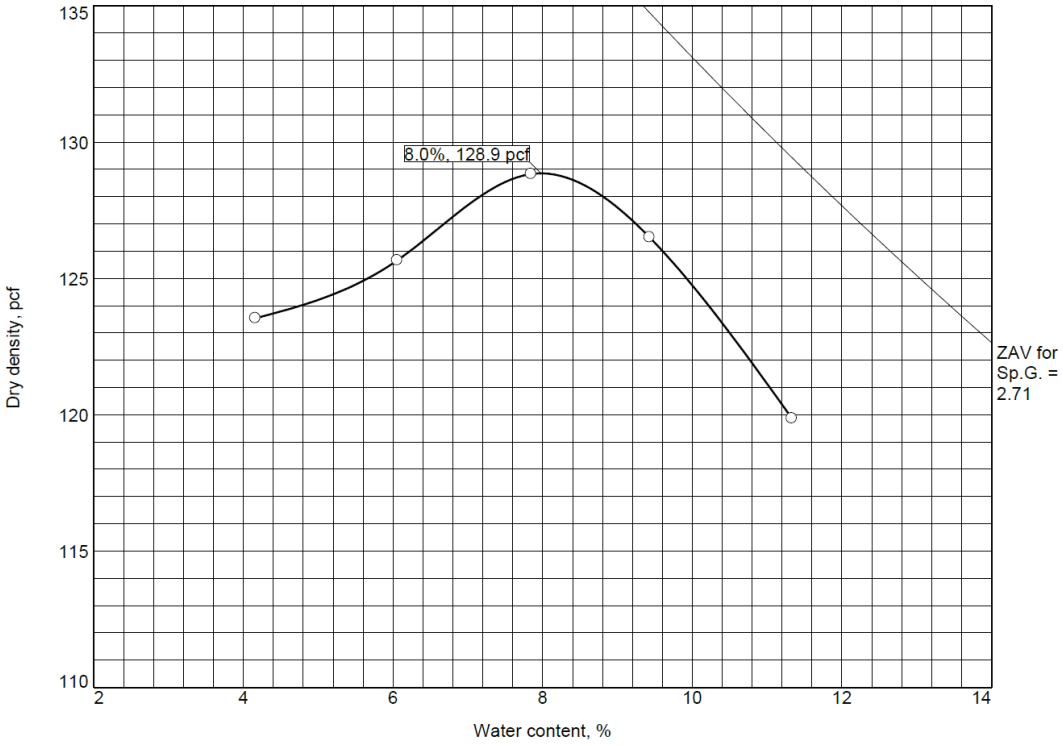

2.2.5 Lean clay

A locally sourced soil classified as a low-plasticity clay (CL) by the USCS was used as the subgrade material. The subgrade material was compacted to prepare a consistent subgrade on which the various backfill materials could be placed. Two stockpiles were used for the different test sites. The particle-size distribution reports can be found in the Appendix. The CL material used for Repairs 1 through 4 is shown in Figure A3, and the CL material used for Repairs 5 through 7 is shown in Figure A4.

2.3 Traffic simulation

The C-17 cargo aircraft was selected for traffic simulation in this study based upon previous testing of large crater repairs in which the repairs failed due to inadequate foundation support for the large gross load. All repairs were trafficked with a specially designed multiple-wheel load cart (Figure 4) to simulate the aircraft's traffic. The load cart represented one-half of the main gear of a fully loaded C-17 with six tires (50 in. by 20 in., 20-ply) inflated to 142 psi. The test gear represented 293,500 lb with individual wheel loads of approximately 48,750 lb. During testing, the tire pressure was monitored using a tire pressure gauge and was adjusted if necessary.

Figure 4. C-17 load cart.

A simulated normally distributed traffic pattern was applied to the pavement repairs in a 9-ft-wide traffic area, as shown in Figure 5. Lanes were designed to simulate the traffic distribution pattern, or wander width, of the main landing gear wheels when taxiing to and from an active runway. The width of each lane corresponded to the contact width, 18 in., of a C-17 tire when fully loaded. The normally distributed traffic pattern was simplified for ease-of-use by the load cart operator. Traffic was applied bi-directionally by driving the load cart forward and then backward over the length of the repairs and then shifting the path of the load cart laterally approximately one tire width on each forward path. This

procedure was continued until one pattern of traffic was completed. For the C-17 test area, one pattern resulted in 28 passes or 24 coverages.

Figure 5. C-17 traffic pattern for each repair.

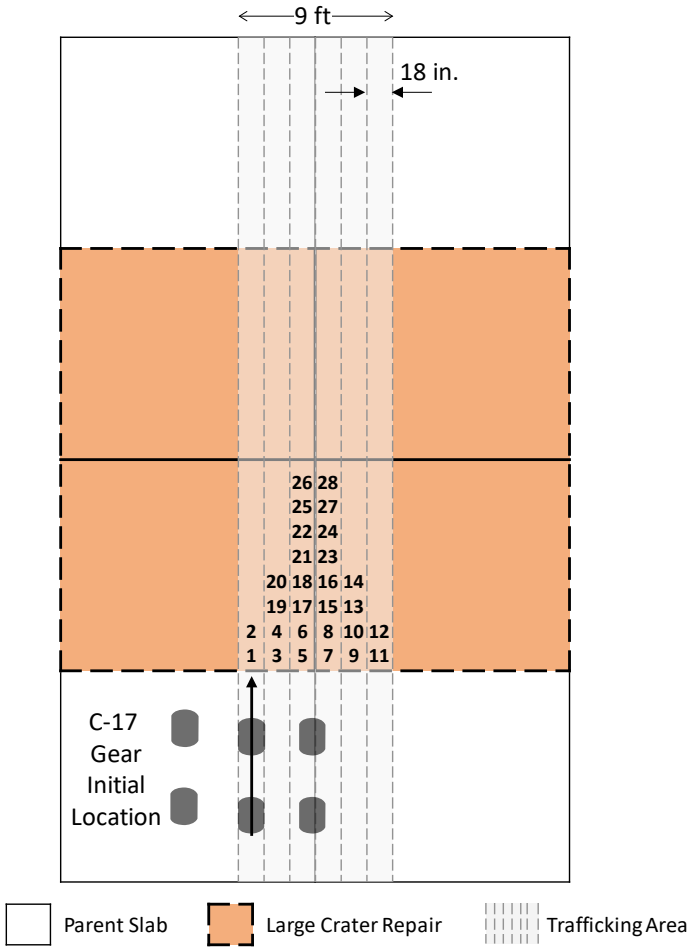

Trafficking operations began approximately 2 hr after the completion of each repair and were continued until failure occurred or 3,500 passes (2,991 coverages) were completed. If the repair sustained 3,500 passes (2,991 coverages), trafficking was discontinued due to time and resource constraints.

2.4 Failure criteria

Visual inspections were performed at selected traffic intervals to identify specific pavement distresses associated with a high foreign object debris (FOD) or tire hazard potential. Distresses were monitored in accordance with traditional condition survey procedures. Structural failure of the concrete pavement was defined as the identification of any

of the following distresses: high-severity shattered slabs or high-severity joint spalling measured by using the pavement condition index (PCI) inspection procedure (ASTM D5340 2018b). If high-severity joint spalls occurred, then the repair was considered functionally failed. Spalling severity was based on the presence of fragmented pieces that might cause FOD or the extent to which the removed pieces of spalled material might cause tire damage hazards. High-severity joint spalls were defined by using their dimensions after FOD was removed.

Joint spalling is produced by excessive stresses at the joint or crack caused by infiltration of incompressible materials or traffic loads. Weak concrete at the joint, which can occur when the concrete is excessively finished during placement, combined with traffic loading also causes spalling. Shattered slabs are intersecting cracks that break the slab into four or more pieces because of overloading and/or inadequate support.

Typical distresses observed in previous experiments with rapid-setting concrete capped repairs included cracking, joint spalling, shrinkage cracks, linear cracks, and shattered slabs. Cracking was considered a minor distress, unless it resulted in the development of associated spalls with an accumulation of loose debris or in crack widths greater than or equal to 1 in. Spalled materials have the potential to damage propellers and rotors of aircraft or be ingested into jet engines. Additionally, spalled concrete and wide cracks present tire hazards due to the potential of the sharp edges to cut aircraft tires.

The concrete repairs were considered failed when distresses posing high FOD potential or tire hazards were identified. For comparative analysis of each repair, failure for this project was quantitatively defined by high-severity shattered slab or joint spalling greater than 2 ft long, 6 in. wide, and 2 in. deep. As FOD was produced during trafficking, it was removed to prevent tire hazards. Loose material in spalls was removed if it could easily be dislodged by hand or broom.

2.5 Data collection

Prior to trafficking, the surface of each repair was inspected for any pre-traffic distresses. After 112 passes (96 coverages), the surface of each repair was inspected again. The 112-pass level represents four traffic patterns with the C-17's six-wheel gear. The repairs were then inspected at approximately 100- to 500-pass intervals (85 to 427 coverages) until

they failed or until 3,500 passes (2,991 coverages) were completed. Cracks were marked using paint crayons, and photographs were taken to document the crack/failure progression.

Each repair was also surveyed by using a rod and level and tested by using a heavy-weight deflectometer (HWD) prior to trafficking, at 112 passes (96 coverages), and after final trafficking (Figure 6). The survey data were used to measure any permanent deformation that occurred. The HWD data provided insight into the stiffness modulus of the pavement structure as the traffic count increased. The HWD data were collected at the center of each quadrant for each repair.

Figure 6. HWD testing on a large crater repair.

Four core samples were extracted from each large crater repair after trafficking was completed. The core samples were used to verify surface thickness and to test the compressive strengths of the rapid-setting concrete. Figure 7 and Figure 8 show the data collection locations for surveying and core sample extractions on the large crater repair areas.

Figure 7. Survey and core sample extraction locations for Repairs 1 through 4.

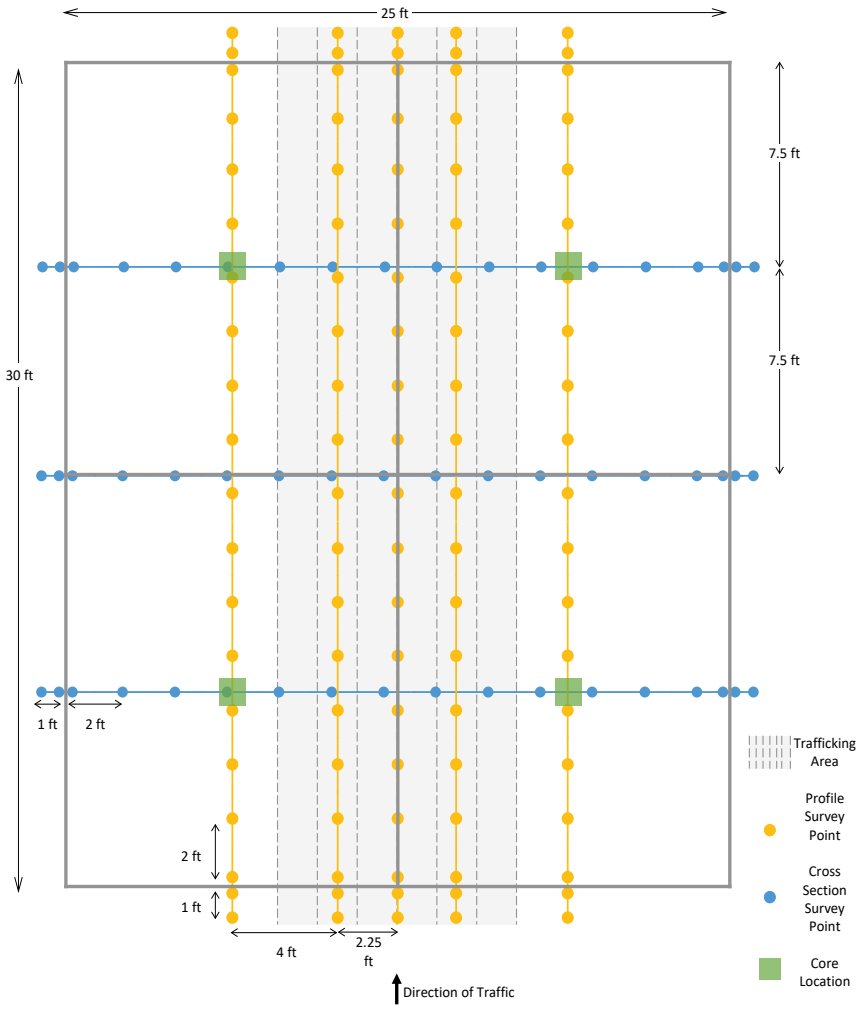

Figure 8. Survey and core sample extraction locations for Repairs 5 through 7.

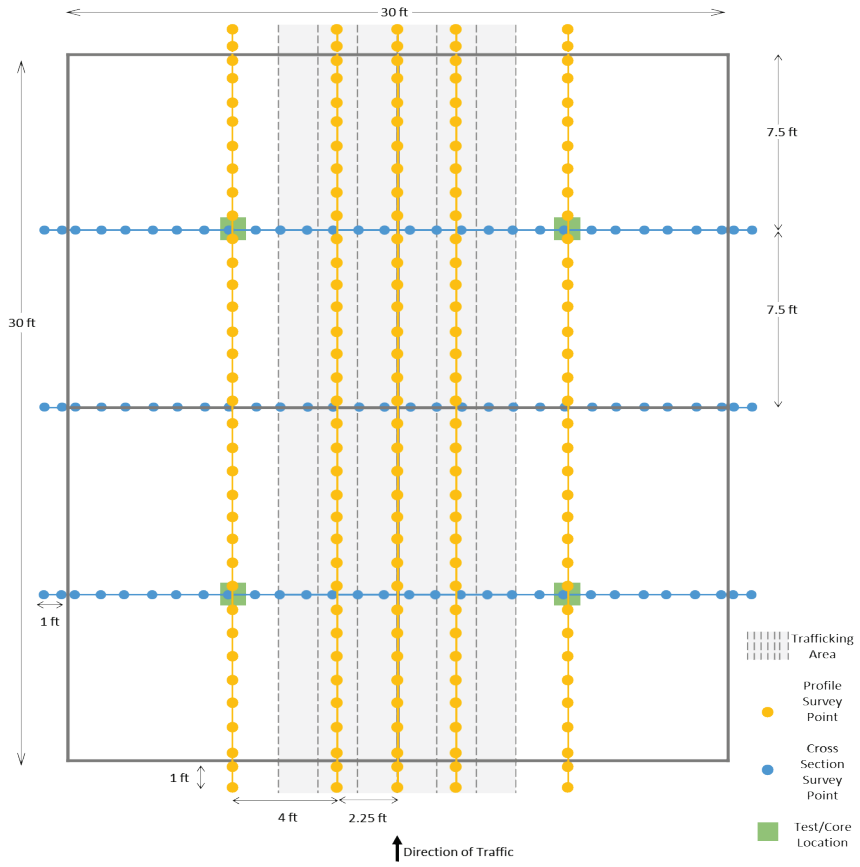

3 Repair Procedures

The same general procedure was used for all repairs, including concrete pavement breaking, sublayer excavation, sublayer-material placement, and rapid-setting concrete surface placement. Each task was accomplished over a period of several days for each repair. Repairs 1 through 4 used one repair area that was 25 ft by 30 ft. Repairs 5 through 7 used a different repair area that was 30 ft by 30 ft. This chapter briefly describes the repair processes used for each repair.

3.1 Concrete breaking

The large crater repairs were formed by breaking and removing the original PCC from four adjacent slabs to create either a 25-ft by 30-ft repair for Repairs 1 through 4 or a 30-ft by 30-ft repair for Repairs 5 through 7. The PCC was broken using a Bobcat E45 mini excavator (Figure 9). Two people were utilized to complete breaking operations, an operator and a spotter, to ensure that the operator did not damage the surrounding PCC slabs. Figure 9 shows the breaking of the PCC surface.

Figure 9. Breaking the PCC surface of the parent slabs.

3.2 Sublayer excavation

Following pavement breaking activities, each repair area was excavated to remove the broken PCC and underlying material. A Bobcat E45 mini excavator with a bucket attachment was used to excavate each repair. An equipment operator and a spotter were used to complete excavation activities. Figure 10 shows the excavating process.

Figure 10. Excavating a repair with a mini excavator.

3.3 Sublayer material placement

Following the excavation of the repair, the existing silty clay (CL) subgrade material was replaced with a low-plasticity clay material obtained from a local source. The material was placed in 6- to 8-in.-thick lifts and compacted with a jumping jack compactor to a target subgrade strength of 15 to 25 CBR. On average, 12 to 18 in. of subgrade material was replaced to ensure consistency between repairs within the test section.

After the subgrade material was compacted, a 6 oz/yd^2 non-woven needle-punched geotextile was placed to ensure material separation of the high-quality limestone base course and subgrade material (Figure 11). For the

limestone base course placement, the layers were compacted in 3- to 4-in.-thick lifts with two coverages of a compact track loader (CTL) with a roller compactor attachment, the CV18B (Figure 12, left), to reach a target strength of 50 or 80 CBR, depending upon the repair objectives. A plate compactor (JPC-80) was used to create a smooth final surface (Figure 12, right). Two technicians were used for compacting the limestone: a CTL operator and a plate compactor operator who was also used as a spotter.

Figure 11. Geotextile placement over the subgrade for crushed limestone base courses.

Figure 12. Compaction of crushed limestone base with the roller attachment (left) and plate compactor (right).

For placing the rapid-setting flowable fill, an extendable boom forklift was used to lower a super sack over the repair void, and the material was dispensed directly into the excavation in thin lifts. Approximately 40 gal of

water per super sack was dispensed over the surface of each lift by using a water truck, a 2-in.-diam hose, and an in-line flow meter. Water was placed so that moisture remained over the material to ensure the next lift was adequately bonded to the existing lift. This process was repeated until the target backfill depth was achieved. For the final lift of flowable fill, typically only 30 to 35 gal of water was dispensed to reduce the amount of standing water on the surface of the flowable fill.

Figure 13 shows the placement process. Typically, six to eight team members were used to place the rapid-setting flowable fill backfill: two forklift operators, three to five laborers to move material, and a water hose/truck operator. Placing 14 in. of rapid-setting flowable fill in 3- to 4-in.-thick lifts with eight team members took 2 hr and 35 min.

Placing 14 in. of rapid-setting flowable fill in 2-in.-thick lifts with eight team members took 3 hr and 35 min. The placement of 2-in.-thick lifts was evaluated to determine if this method would reduce dry material pockets, producing a homogenous flowable fill mixture. However, the 2-in.-thick lifts were more time-consuming and meticulous and were found to not be necessary for achieving a full-strength flowable fill base.

A wooden board was utilized to ensure the targeted thickness of the rapid-setting flowable fill material was achieved (Figure 14). The flowable fill backfill for Repair 1 was placed approximately 2 weeks prior to the surface placement due to the Thanksgiving holiday break and weather. The flowable fill backfill for Repair 3 was placed 24 hr prior to the surface placement.

A fire-hose-type nozzle was originally used for flowable fill in Repair 1 (Figure 13d). This nozzle dispensed the water too rapidly, forcing the water to run downhill too quickly without percolating into the flowable fill at the higher elevations. A shower-type nozzle was used for Repair 3 to disperse the water out of the hose in a more wide-spread, less forceful pattern (Figure 15). Therefore, the water percolated into the flowable fill at an even, steady rate. It is important to note that for large crater repairs, water should be placed at the higher elevations first, since the water would naturally gravitate towards the lower elevations.

Figure 13. Rapid-setting flowable fill placement process.

(a) Mobilizing super sacks of flowable fill

(b) Dispensing dry material

(c) Adding water to dry flowable fill

(d) Ensuring water coverage

(e) Spot checking flowable fill depth

(f) Final surface

Figure 14. Wooden board to ensure targeted flowable fill depth.

Figure 15. Shower-type nozzle used for dispensing water over dry flowable fill.

For the cement-stabilized silty sand base course material, 18 bags of Type 1 cement were strategically placed on top of a 25-ft by 21-ft by 1-ft-high area of silty sand for each of the four lifts of cement-stabilized silty sand as shown in Figure 16. This layout was used to obtain a 5% cement by dry weight of soil blend. A Caterpillar LT13B CTL tiller attachment (Figure 17) was used to mix the cement and soil. A front-end loader (Komatsu WA150) was used to flip the soil to ensure the soil on the bottom was incorporated with the cement. The mixing process for each lift took approximately 20 min.

Figure 16. Cement layout on top of silty sand for strategic mixing.

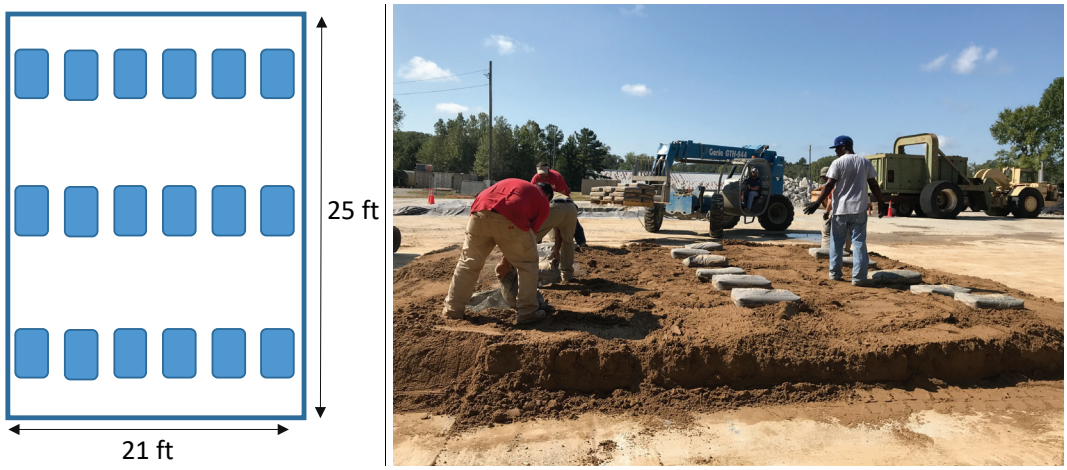

Figure 17. Tiller attachment mixing cement with silty sand and flipping soil with front-end loader.

The cement-stabilized silty sand was placed in two 4-in.-thick compacted lifts and two 3-in.-thick compacted lifts to obtain a total thickness of 14 in. The treated soil was placed by using the front-end loader, shovels, and rakes. Each treated soil lift was placed 2 to 3 in. more than the desired level to account for compaction. The first three lifts were compacted with two passes of the jumping jack, and the final lift was compacted with four passes of the jumping jack. Two jumping jacks, a Wacker Neuson BS70-4 and a Multiquip Mikasa MTX70 HD Rammer were used to compact the mixed soil (Figure 18). One pass of compaction was completed by starting in one corner and moving the jumping jack around the perimeter of the repair until it reached the center of the repair.

Figure 18. Jumping jack compaction.

3.4 Expedient formwork

It is difficult to place large sections of rapid-setting concrete at one time due to the quick-setting nature of the material. Formwork comprised of 12-ft-long plasticPoly Meta Forms® and expansion boards was required to divide the repair into quadrants to create four smaller placements when capping the surface with rapid-setting concrete. The quadrants helped the volumetric mixer to not exceed its workable limits and also to ensure a quality repair. The plastic forms included steel slide pockets for connecting the forms.

The formwork was placed directly on top of the base course layer. Two heights of forms were used, 4 in. and 6 in., depending upon the targeted surface thickness. The forms were stacked to create a total height that was approximately 2 in. less than the targeted rapid-setting concrete thickness. The formwork was cut to the length of the repair with a sawzall and placed so that the top of the form was level with the top of the parent slab and a small gap remained between the bottom of the form and top of the base. This small gap was necessary so that the forms could be quickly and easily adjusted to match the grade of the adjacent parent slabs. The gap at the bottom of the form was temporarily filled with crushed limestone to prevent the rapid-setting concrete from flowing into the other quadrants. No expansion boards or dowels were used between the repaired slabs and the parent slabs.

A stringline was used to ensure the grade matched with the neighboring parent slabs. To join the forms and set them in place, ¾-in.-diam, 24-in.-long stakes were hammered into the base through the slide pockets (Figure 19).

Slide pockets and stakes were placed approximately every 3 ft along the forms for stability.

Forms were installed so that two quadrants, positioned diagonally from each other, could be capped with rapid-setting concrete without removing forms (Figure 20). Only after the first two quadrants were placed were the forms removed to prepare for the application of expansion boards.

Figure 19. Staking forms.

Figure 20. Form placement.

Expansion joint boards were used only between the repair slabs and not between the repair slabs and the parent slabs. Several options of installing the joint boards between the repairs were studied during this project. It was desired to have a quick application method with strong installation materials.

Repairs 1 and 2 used a combination of heavy-duty multi-purpose construction adhesive (Liquid Nails Construction Adhesive) and #9 x 1.5-in. fluted masonry nails (Figure 21). The adhesive was applied to the joint board, which was held into place by hammering the masonry nails into the repair while the adhesive set. The nails had to be hammered into the fresh rapid-setting concrete repair after the initial set but before completely cured. It was found that the nails popped out easily because they were not long enough, and the Liquid Nails did not readily adhere to the dusty concrete. The foam joint board had to be forced in place by multiple people as the Liquid Nails hardened. The timing of the joint board placement was not recorded. The method worked; however, it was not conducive to a fast-paced theater of operations environment.

Figure 21. Installation of expansion board that included a combination of applying Liquid Nails and masonry nails in the curing rapid-setting concrete (Repair 1).

Three additional types of adhesive were tested on Repair 3 – CTS Adhesive, Loctite Foamboard (PL300), and Power Grab. The CTS Adhesive was applied on the foam board by using a caulk gun. The foam board was then placed on the curing concrete of one side of a repair quadrant, where it stayed in place immediately after the initial force of the installation. The total process for the one 15-ft-long side was 3 min. Loctite Foamboard was also applied to the foam joint board of one Repair 2's quadrants by using a caulk gun. The foam board adhered to the concrete almost immediately; however, it was not as secure. This process also took 3 min. A caulk gun was not required for the application of Power Grab. The material was applied to the joint board and placed on one of the 15-ft-long curing concrete walls. The glue material was not strong enough to keep the foam board in place. The process took 3 min.

Repair 3 also used the Opperman Method on two of the 15-ft-long plastic forms. The Opperman Method, demonstrated in Figure 22, consisted of attaching foam joint board to the plastic forms by using duct tape and screws. This process was completed when the plastic forms were installed before the rapid-setting concrete placement began. The foam board was cut to fit the plastic form length, and duct tape was wrapped around the forms and foam board every 2 to 3 ft. Three-inch-long screws were inserted in the foam joint board where the duct tape was placed, but care was taken to ensure the screws did not penetrate the plastic forms. The screws were 3 in. long so that the rapid-setting concrete could form around the screws and cure (Figure 23). Three people executed the Opperman Method of taping the joint boards to the forms and inserting screws in approximately 3 min.

When the concrete was just set but still curing, the tape was cut away at the top and bottom of the foam board so that the plastic forms could be removed before the remaining two quadrants were filled with rapid-setting concrete. With this Opperman Method, there was no wait time as with using adhesives to attach the foam joint boards.

Figure 22. The Opperman Method - attaching expansion board to plastic forms with duct tape (left) and inserting screws (right).

Figure 23. Close-up view of the finished Opperman Method.

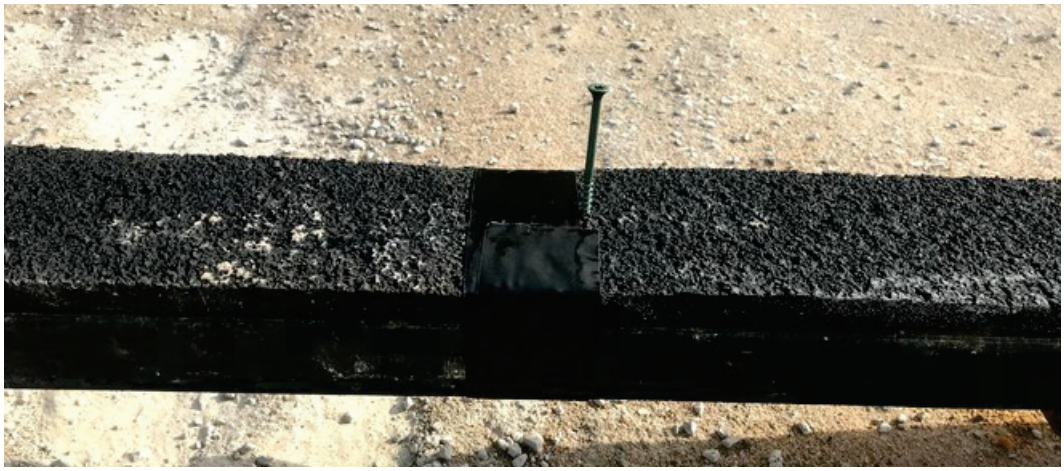

Two additional adhesives were applied with a caulk gun in Repair 4. Loctite PL Pro Line Premium Construction Adhesive and Gorilla Heavy Construction Adhesive were placed in the same manner to the foam board and pressed onto the curing concrete. Neither product was strong enough to hold the foam board in place. A spray contact adhesive, 3M Hi-Strength 90, was then tested on Repair 4 (Figure 24) and was also ineffective at adhering to the newly placed rapid-setting concrete. The Opperman Method was then used for Repair 4 as well as Repairs 5, 6, and 7.

Figure 24. Spray adhesive on expansion board.

3.5 Rapid-setting concrete placement

Following the placement of the foundation materials, each repair was capped with CTS Rapid Set Concrete Mix®. A simplified volumetric mixer, factory calibrated for the repair material and manufactured by CemenTech Inc. (www.cementech.com), was used for all repair capping activities. Prior to each repair, six to seven 3,000-lb super sacks of the rapid-setting concrete mix were loaded into the volumetric mixer. Each water tank on the simplified volumetric mixer was also filled during this time with approximately 250 gal of water. Approximately 12.5 lb of citric acid was added to each water tank when the air temperatures were above 85°F.

Before placement of the concrete cap, the repair void, including the saw-cut faces and sublayer material, was dampened by using the pressure washer attachment on the mixer. All parts of the volumetric mixer and the plastic forms were sprayed with a form-release agent prior to starting the repair process. The rapid-setting concrete was then dispensed directly into the repair void, taking care to adjust the water volume, as needed, to produce a

somewhat high-slump concrete. The wet mix was targeted to make screeding easier. Once the repair was filled, the concrete cap was screeded once or twice. Minimal hand finishing, if needed, was applied to the surface of the repairs by using hand trowels. Care was made to clean the excess material from around the repair area to prevent FOD during trafficking.

Figure 25 and Figure 26 show the placement of the rapid-setting concrete surface using the simplified volumetric mixer. The material was moved with concrete rakes to the end of the repair with the higher elevation. As shown in Figure 27, the rapid-setting super sacks were lined up close to the repair, ready to be loaded into the volumetric mixer continuously because of the quick-setting nature of the material. Each 10-in.-thick repair used approximately 30 super sacks. The 6-in.-thick repair used 20 super sacks, and the 14-in.-thick repair used 36 super sacks.

Figure 28 shows the rapid-setting concrete surface after screeding was almost completed. For Repairs 1 through 4, a 20-ft-long magnesium bar (Figure 28) was used to screed the repairs. For Repairs 5 and 6, a prototype forklift screed called the Autoskreed Telehandler (ASTH) was used as shown in Figure 29, and for Repair 7, a modified, improved prototype forklift screed called the RADR Screed was used as shown in Figure 30 (Cox et al. draft*). Typically after screeding, the excess rapid-setting concrete material is cleaned from the outside of the repair by using hand trowels as shown in Figure 31.

* Cox, B. C., N. R. Hoffman, and T. A. Carr. *Evaluation of a prototype integrated pavement screed for screeding asphalt or concrete crater repairs*. ERDC/GSL TR (draft). Vicksburg, MS: U.S. Army Engineer Research and Development Center.

Figure 25. Placing rapid-setting concrete.

Figure 26. Close-up of placing rapid-setting concrete.

Figure 27. Super sacks of rapid-setting concrete lined up prior to starting repair.

Figure 28. Screeding with 20-ft-long magnesium bar.

Figure 29. Prototype screed, the Telehandler Autoskreed (ASTH).

Figure 30. Modified prototype screed, RADR Screed.

Figure 31. Cleaning excess material from outside of the repair.

Because of the large repair volume, the volumetric mixer required regular washing out (Figure 32) between quadrants. The volumetric mixer was rinsed with a pressure washer, and the auger was completely cleaned (Figure 33). The washout after every quadrant ensured that the mixer did not clog and lock up.

Figure 32. Refilling volumetric mixer water tanks (background).

Figure 33. Washout of volumetric mixer using a pressure washer (left) and the resulting clean auger (right).

Eight to nine people were utilized for capping including a vehicle operator, a mixer operator, a forklift operator, a person to help with loading bags on the forklift, and four to five additional personnel for spreading material and screeding. Each repair surface was allowed to cure for approximately 2 hr prior to the application of traffic. The 2-hr cure time had previously been identified for expedient repair efforts with this material (Priddy 2011).

3.6 Parent slab replacement and patches

Two of the existing parent slabs on the test section next to the area (west end) for Repairs 1, 2, 3, and 4 had some minor damage. So, the two adjacent slabs were replaced with 13 in. of PCC prior to the crater repair testing. However, pavement distresses in the form of joint spalls were noted on the west-end parent slabs after 2,000 passes (1,709 coverages) of the C-17 load cart on Repair 1 were applied. The joint spalls steadily increased in severity as Repairs 2 and 3 were trafficked. The joint spalls were repaired with small patches prior to the start of Repair 5 as shown in Figure 34. The damage to the parent slabs did not seem to have an effect on the pavement condition of the crater repairs.

Figure 34. Patching high-severity joint spalls on the parent slabs adjacent to the repair area.

The parent slabs adjacent to the repair slabs in the direction of traffic (east and west ends) for Repairs 5 and 6 received some damage during trafficking. Parent slab damage was noted after the trafficking of Repair 5. The damage on the parent slabs on the west end of the repair had largely increased after Repair 6 was trafficked. Therefore, the two parent slabs on the west end of the repair area were replaced and cured before Repair 7 began. The 6-in.-thick limestone base course under the parent slabs was compacted, and 15 in. of PCC was placed.

3.7 Quality assurance tests

Several tests were conducted to ensure that each repair layer was constructed to its target layer thickness and that similar subgrade and base strengths were achieved between repairs. This included semi-destructive testing of the sublayer materials, nuclear gauge testing, and surveying the surface elevation of each repair layer.

3.7.1 Dynamic cone penetrometer (DCP)

After compaction of the subgrade, four DCP tests were conducted to determine the DCP-estimated CBR values for the subgrade following the procedure described by ASTM D6951 (2018c). The DCP tests were conducted in the center of each quadrant. A CBR value ranges from 0 to 100%, and a CBR value of 100% is equivalent to the bearing capacity of a compacted, dense-graded, crushed aggregate. After compaction of the base, three additional DCP tests were conducted to determine the strength of the base material. Results of DCP testing prior to trafficking are presented in Table 2.

Table 2. Average CBR data of sublayers measured using DCP prior to trafficking.

Repair No.	Target Surface Thickness (in.)	Base Material	Target Base Thickness (in.)	Average Base CBR (%)	Subgrade Material	Average Subgrade CBR (%)
1	10	Rapid-Setting Flowable Fill	14	100	Lean Clay	25
2	10	Crushed Limestone	14	65	Lean Clay	15
3	6	Rapid-Setting Flowable Fill	14	100	Lean Clay	25
4	10	Crushed Limestone	20	50	Lean Clay	20
5	10	Crushed Limestone	20	85	Lean Clay	25
6	14	Crushed Limestone	16	100	Lean Clay	25
7	10	Cement-Stabilized Silty Sand	14	75	Lean Clay	15

For a course-grained material such as the limestone base used in this test section, Webster et al. (1994) determined that a 5-in.-minimum penetration depth was required before the actual strength of the surface soil layer could be determined with the DCP. The crushed limestone base layers of the repairs were 14 to 20 in. thick, so the DCP data from only the bottom 9 to 15 in. of the material was used to estimate CBR.

After trafficking of each repair was completed, three additional DCP tests were conducted to determine whether any changes in foundation strength occurred. Forensic DCP tests were conducted by drilling a 1-in.-diam hole through the Rapid Set Concrete Mix® surface and testing with the DCP through the base and subgrade layers. Results of DCP tests conducted after trafficking are presented in Chapter 4.

3.7.2 Nuclear density gauge tests

Table 3 shows the results of nuclear density gauge tests (ASTM D6938 2017d) for each constructed layer. The soil base and subgrade layers were tested with a nuclear density gauge at four different test points within each repair, typically the center of each quadrant. The gauge was then turned 90 deg at each test location for a second measurement at the same test point.

Table 3. Nuclear density gauge-measured layer properties as constructed.

Repair No.	Base					Clay Subgrade		
	Material	Thick-ness (in.)	Average Moisture (%)	Average Dry Density (lb/ft³)	Average Wet Density (lb/ft³)	Average Moisture (%)	Average Dry Density (lb/ft³)	Average Wet Density (lb/ft³)
1	Rapid-Setting Flowable Fill	14	n/a	n/a	n/a	15.2	112.4	129.4
2	Crushed Limestone	14	4.2	134.2	139.7	15.2	112.4	129.4
3	Rapid-Setting Flowable Fill	14	n/a	n/a	n/a	17.0	87.1	101.9
4	Crushed Limestone	20	2.8	130.2	133.8	12.1	121.2	135.9
5	Crushed Limestone	20	3.2	139.4	144.2	15.3	102.7	118.4
6	Crushed Limestone	16	3.0	130.5	134.5	15.3	102.7	118.4
7	Cement-Stabilized Silty Sand	14	7.9	121.5	131.2	10.7	98.1	118.6

3.7.3 Surveying

A rod and level were used to verify that the target layer thicknesses for each sublayer and the repair caps were achieved. Surveying was accomplished within the repair area, as shown in Figure 7 and Figure 8. Five lines of points were collected in the direction of traffic on each repair. Three lines of points were collected for the cross-section measurements. Additional data were collected at the repair joints to determine elevation changes at the joint due to removal of spalled material during trafficking. Layer thickness values for each repair are presented in Table 4. All pavement layers were constructed within 1 in. of the targeted thicknesses.

Table 4. Target and actual layer thicknesses.

Repair No.	Concrete Surface		Base		
	Target Thickness (in.)	Average Thickness (in.)	Base Material	Target Base Thickness (in.)	Average Base Thickness (in.)
1	10	11	Rapid-Setting Flowable Fill	14	13.5
2	10	10	Crushed Limestone	14	14
3	6	6.5	Rapid-Setting Flowable Fill	14	13.5
4	10	10.5	Crushed Limestone	20	20
5	10	10.5	Crushed Limestone	20	20
6	14	14	Crushed Limestone	16	16
7	10	10	Cement-Stabilized Silty Sand	14	13.5

4 Repair Performance Results

Table 5 presents the overall results of the C-17 traffic testing of the large crater repairs. As mentioned previously, trafficking was discontinued after 3,500 passes (2,991 coverages) if failure had not occurred. The following sections describe the results for each repair, including the surface distresses and pavement structure forensics data. The mode of failure for all seven repairs was high-severity spalling along the transverse joints (joints perpendicular to the direction of travel). Since spalling produces FOD, the overall FOD potential for the repairs was also monitored and removed periodically.

Table 5. Trafficking results of rapid-setting concrete large crater repairs.

Repair No.	Surface Thickness (in.)	Base Material	Base Thickness (in.)	C-17 Passes to Failure[a]	Failure Mode
1	11.0	Rapid-Setting Flowable Fill	13.5	3,500	Tire Hazard[b]
2	10.0	Crushed Limestone	14.0	100	Joint Spalling
3	6.5	Rapid-Setting Flowable Fill	13.5	450	Joint Spalling
4	10.5	Crushed Limestone	20.0	225	Joint Spalling
5	10.5	Crushed Limestone	20.0	225	Joint Spalling
6	14.0	Crushed Limestone	16.0	1,600	Joint Spalling
7	10.0	Cement-Stabilized Silty Sand	13.5	900	Joint Spalling

[a] Failure was defined as a joint spall that is at least 2 ft long, 6 in. wide, and 2 in. deep; a high-severity shattered slab; or a tire hazard.

[b] Largest joint spall at 3,500 passes was 63 in. long, 3.5 in. wide, and 3.25 in. deep; shape and depth of spall created off of interior corner break created a tire hazard.

4.1 Surface distresses

4.1.1 Repair 1

Repair 1 had the best performance of all repairs. Repair 1, with an 11-in.-thick rapid-setting concrete surface and a 13.5-in.-thick rapid-setting flowable fill base course, failed at approximately 3,500 passes (2,991 coverages) due to a tire hazard. The repair had a joint spall that was 63 in. long and 3.25 in. deep; however, the width of the spall was 3.5 in. wide, which did not meet the defined failure criteria. In RADR scenarios, pavement deterioration limits would be expected to exceed peace-time standards due to the critical nature of the mission. Since the width of this spall was less than the failure criteria defined for this

research, it would be expected that the aircraft tires could bridge over the spall with minimal risk to the aircraft. The progression of distresses with increasing traffic can be found in Figure 35.

Figure 35. Repair 1 progression of distresses.

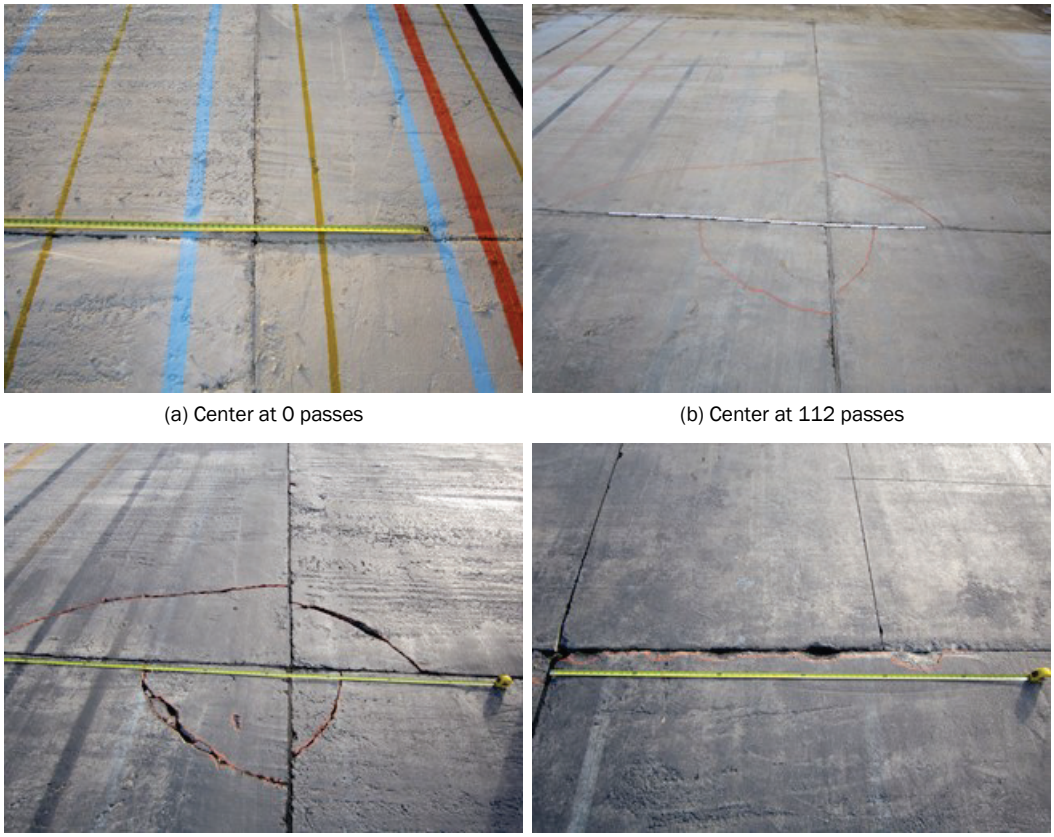

(a) Center at 0 passes

(b) Center at 112 passes

(c) Center at failure, 3,584 passes

(d) Spalling at failure, 3,584 passes

Repair 1 was trafficked with the C-17 load cart 2 hr after the fourth quadrant was placed to demonstrate the rapid return to service for a RADR scenario. Figure 35 shows that there were no cracks prior to trafficking. Cracking began around 56 passes (48 coverages). After 112 passes (96 coverages), low-severity corner breaks were observed at the center of the repair in each quadrant, which formed somewhat of a circle, as shown in Figure 35. This is indicative of inadequate foundation support and is consistent with prior testing of large craters (Barna et al. 2010).

Low-severity joint spalling on the outer-trafficked edges was observed after 250 passes (214 coverages). The measured FOD was at a maximum size of 0.5 in. After 448 passes (383 coverages), two of the center corner breaks began spalling with 1.25-in.-sized maximum FOD. The joint

spalling on the trafficked edges and the interior corner breaks began steadily progressing after 672 passes (574 coverages), creating approximately 1.5-in.-sized FOD. After 1,680 passes (1,436 coverages), the FOD size increased to an average of 2 in. (Figure 36). While the FOD generated during the traffic testing was undesirable, it is recognized that an active airfield sweeping program would be expected to remove the material between aircraft operations and additional operational risk would be assumed in a RADR scenario.

Figure 36. Large 2-in. FOD after 1,680 passes, in the center of Repair 1.

Trafficking was stopped after 3,584 passes (3,063 coverages) due to a tire hazard on one of the interior corner breaks, which was approximately 3.25 in. wide and 3.25 in. deep (Figure 35 [c] and Figure 37). Figure 35 (d) shows the spalling on the east edge at 3,584 passes (3,063 coverages).

The parent slabs surrounding the repair on the west edge began spalling around 1,680 passes (1,436 coverages), as shown in Figure 38. The 13-in.-thick parent slabs were made with a 5,000-psi high-quality airfield PCC mixture and were placed 5 months before Repair 1 began. Crushed limestone was used as the base course material for the parent slabs. These data show that the performance of Repair 1 exceeded that of ordinary plain concrete pavement construction for the conditions noted.

Figure 37. Measuring center crack depth.

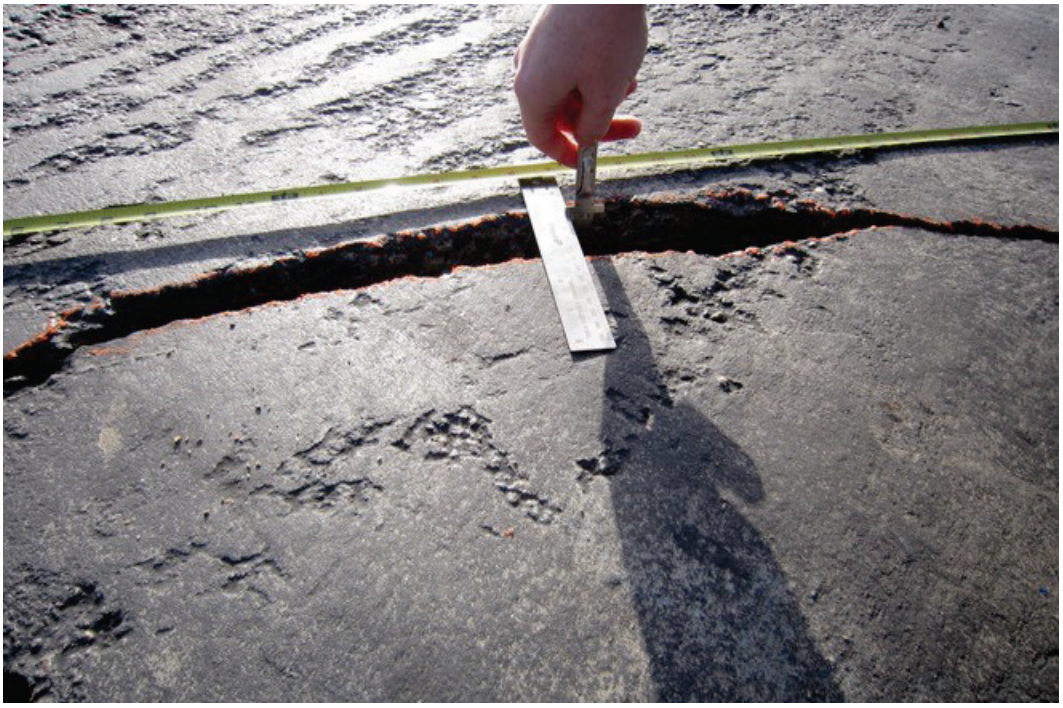

Figure 38. Parent slabs adjacent to the repair started to spall after 1,680 passes.

4.1.2 Repair 2

The rapid-setting concrete surface and crushed limestone base course thicknesses were 10 and 14 in., respectively, for Repair 2. Failure of the repair occurred after approximately 100 passes (85 coverages) due to a high-severity joint spall on the western edge. The repair was also close to failure on the eastern edge due to a high-severity joint spall. The progression of distresses with increasing traffic can be found in Figure 39.

The repair had a few shrinkage cracks on the surface that were observed prior to trafficking (Figure 40). The shrinkage cracks appeared on the surface soon after each quadrant was placed. Linear cracks and interior corner breaks were observed on the surface after just 18 passes (15 coverages). After 112 passes (96 coverages), the repair was shattered in three of the four quadrants, and high-severity joint spalling was observed on the trafficked edges; the repair exceeded the failure criteria. A tire hazard was not present, so the repair was trafficked beyond failure for assessment. After 224 passes (191 coverages), the dimensions of the joint spalls had not progressed from dimensions measured at 112 passes (96 coverages). However, spalling on the parent slabs along the western edge of the repair had occurred (Figure 41). The center of the repair was cracked in a circular shape (interior corner breaks) at 224 passes (191 coverages), as shown in Figure 42. The interior corner breaks indicate that the combination of the slab thickness and foundation strength/thickness was inadequate to support the heavy load.

Figure 39. Repair 2 progression of distresses.

(a) Overview of repair at 0 passes

(b) Low severity shattered slab at 112 passes

(c) FOD and spall on the western edge at 112 passes

(d) FOD on the eastern edge at 112 passes

(e) Spall on the western edge at 224 passes

(f) Spall on the eastern edge causing failure at 224 passes.

Figure 40. Minor shrinkage cracking at 0 passes.

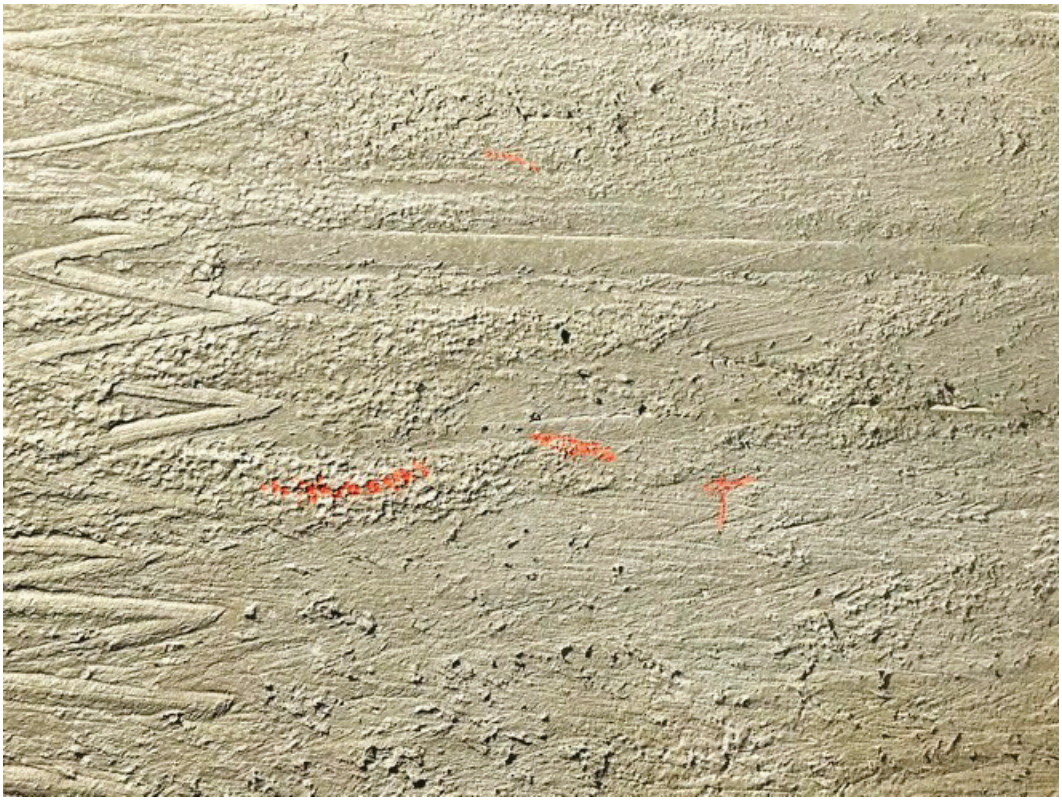

Figure 41. Spalling on parent slab in the trafficking area at 224 passes.

Figure 42. Cracking in the center of Repair 2 at 224 passes.

4.1.3 Repair 3

Repair 3, with a 6.5-in.-thick rapid-setting concrete surface and a 13.5-in.-thick rapid-setting flowable fill base layer, failed at approximately 450 passes (385 coverages). The mode of failure was spalling on the transverse joints. The maximum spall size was 106 in. long, 11 in. wide, and 2 in. deep. The observed FOD was between 1 and 2 in. A few shrinkage cracks were noted prior to traffic; however, they had no effect on the repair failure. The progression of distresses with increasing traffic can be found in Figure 43.

Figure 43. Repair 3 progression of distresses.

(a)) Overview of repair at 0 passes

(b) Joint spall in Quadrant #1 at 112 passes

(c) Cracking in center of repair at 448 passes

(d) Failed eastern trafficked edge spall at 448 passes

After 112 passes (96 coverages), a 12-in.-long joint spall was noted at the interior northwest joint. Several more joint spalls, interior corner breaks, and linear cracks were created on three of the four quadrants by the time the repair received 336 passes (287 coverages) with the C-17 load cart. After 392 passes (335 coverages), all quadrants had joint spalling along the trafficked edges; however, corner breaks and linear cracks were still noted on only three of the four quadrants. The joint spalls progressed when failure was noted at 448 passes (383 coverages). Trafficking continued after failure to observe the joint spalling progression. One joint spall created a minimal amount of FOD at 504 passes (431 coverages); however, all existing spalls were not any deeper, wider, or longer than they were at 448 passes (383 coverages).

The rapid-setting flowable fill was placed in 2-in.-thick lifts for Repair 2, rather than the typical 3- to 4-in.-thick lifts. This was done in an attempt to increase the water percolation into the flowable fill. However, as can be seen in Figure 44, after excavation, each lift of the

material appeared to be delaminated. Figure 45 shows that the layers delaminated in the same thickness it was placed.

Figure 44. Rapid-setting flowable fill during the backfill breaking and removal process.

Figure 45. Close-up of flowable fill layers during removal.

4.1.4 Repair 4

Repair 4, consisting of 10 in. of Rapid Set Concrete Mix® over 20 in. of crushed limestone base material, withstood 225 passes (192 coverages) of C-17 load cart traffic before failing. Repair 4 had a few shrinkage cracks develop in one quadrant during the concrete curing process. By

112 passes (96 coverages), cracking occurred at all four interior corners, and multiple linear cracks developed in three of the four quadrants. Two quadrants were classified as low-severity shattered slabs. After 225 passes (192 coverages), all four quadrants were shattered and were more severe than the distresses observed at 112 passes (96 coverages). High-severity joint spalling developed along the western trafficked edge resulting in the repair's failure. The FOD produced from the pavement distresses ranged from 1/8 to 1.5 in. The progression of distresses with increasing traffic can be found in Figure 46.

Figure 46. Repair 4 progression of distresses.

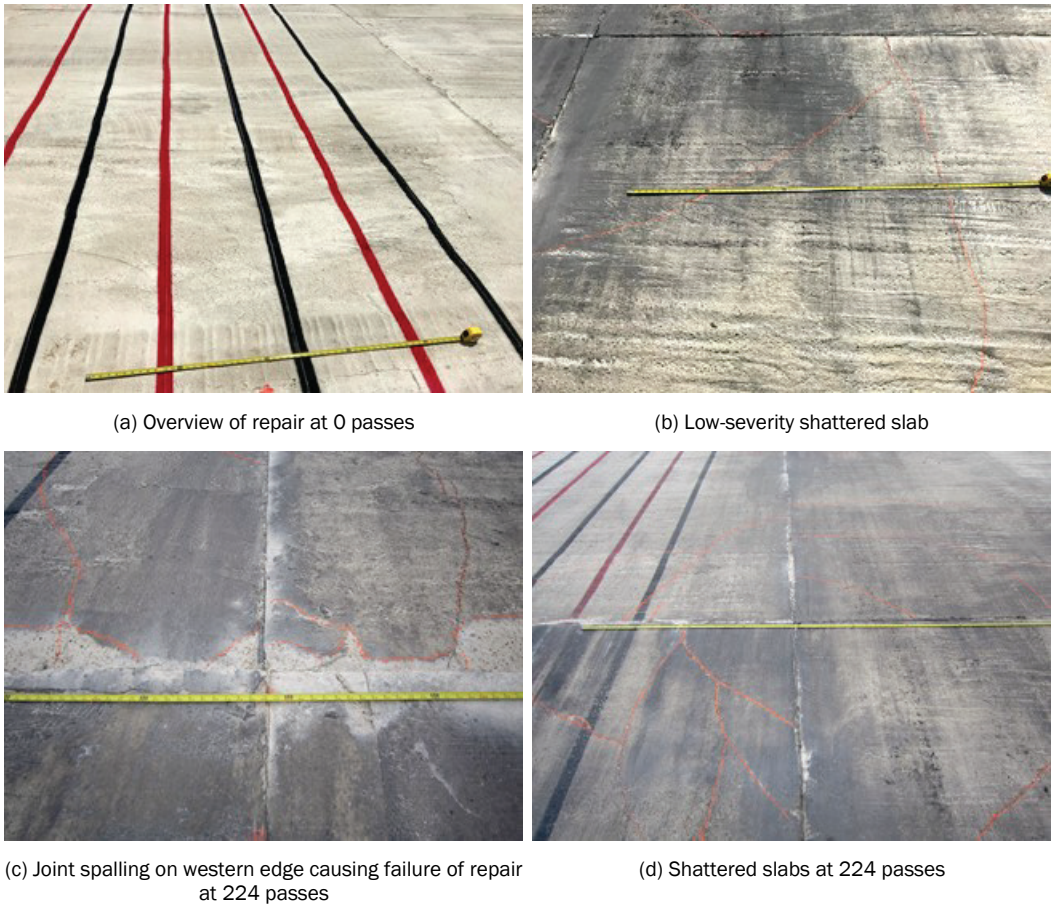

(a) Overview of repair at 0 passes

(b) Low-severity shattered slab

(c) Joint spalling on western edge causing failure of repair at 224 passes

(d) Shattered slabs at 224 passes

Another 112 passes (96 coverages) were applied to the repair after failure. No new cracks developed; however, the pre-existing cracks became more severe (Figure 47). Additional high-severity joint spalling developed along both the eastern and western trafficked edges. After 500 passes (427 coverages), the linear cracks had not progressed in severity; however, the joint spalls did continue to deteriorate.

Figure 47. Western edge of Repair 4 after 336 passes.

4.1.5 Repair 5

Repair 5, consisting of 10.5 in. of Rapid Set Concrete Mix® over 20 in. of crushed limestone, was a repeat of Repair 4 except that the strength of the crushed limestone base course was much higher with a CBR of 100%. Both Repair 4 and Repair 5 failed at approximately 225 passes (192 coverages) due to high-severity joint spalling. Repair 5 seemed to deteriorate at the same rate as Repair 4. This indicates that the base strength may not influence repair performance as much as surface thickness. The progression of distresses with increasing traffic can be found in Figure 48.

All four quadrants of Repair 5 had minimal shrinkage cracks after placement of the rapid-setting concrete surface. After 112 passes (96 coverages), linear cracks developed in two quadrants, but no joint spalling was observed. Traffic was stopped at 224 passes (191 coverages) where three of the quadrants developed low-severity shattered slabs, and both the western and eastern trafficked edges had high-severity joint spalling. The most severe joint spall was 88 in. long, 9 in. wide, and 2 in. deep with 1- to 2-in.-sized FOD and, therefore, the repair was considered failed.

Figure 48. Repair 5 progression of distresses.

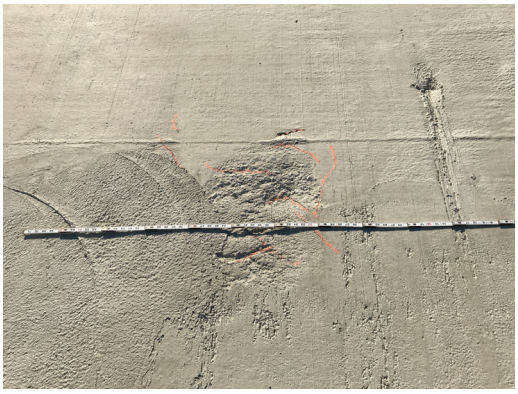

(a) Shrinkage cracking in Quadrant #4 at 0 passes

(b) Low-severity crack at 112 passes

(c) High-severity spall in Quadrant #2 at 274 passes

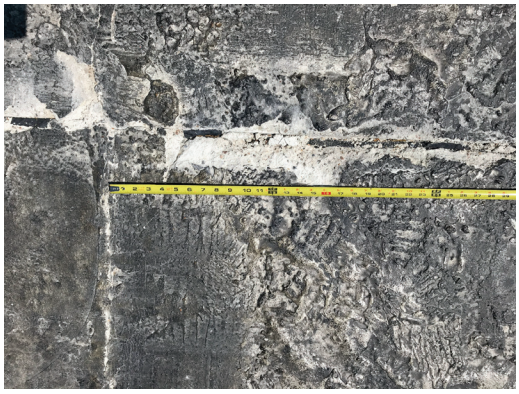

(d) Spalling seen in the center of the repair at 274 passes

Trafficking continued after failure. After 274 passes (234 coverages), no new cracks developed (Figure 49). The joint spalls were slightly more severe. The west side of the repair was more deteriorated than the east side. After 336 passes (287 coverages), the joint spalls and cracking had not progressed significantly, but the parent slabs on the west edge were heavily spalled. The spalling on the western edge can be seen in Figure 49. The parent slab joint spalls did not seem to affect the condition of the repair during trafficking.

Figure 49. Overview of Repair 5 at 274 passes.

4.1.6 Repair 6

Repair 6 had a thicker rapid-setting concrete surface of 14 in. and a 16-in.-thick crushed limestone base. The repair failed at approximately 2,100 C-17 load cart passes (1,795 coverages). The progression of distresses with increasing traffic can be found in Figure 50.

Repair 6 had many shrinkage cracks on the surface that developed during the concrete curing. The Rapid Set Concrete Mix® had a higher slump than desired, causing an approximate 1-in.-thick paste to form on the surface of all quadrants. This paste layer broke during trafficking up to 112 passes (96 coverages) as shown in Figure 51, but the paste layer did not continue to deteriorate after 112 passes.

Joint spalling along a portion of the eastern trafficked edge was noted after 224 passes (191 coverages). A large amount of 0.25-in.-sized FOD was produced from the spall. Joint spalling began to develop and progress starting around 336 passes (287 coverages). Linear cracking was observed after 768 passes (656 coverages). Repair 6 was considered failed at 2,112 passes (1,805 coverages) due to 114-in.-long, 10-in.-wide, and 2-in.-deep spalling along the western trafficked edge (Figure 52). Traffic continued until 2,504 passes (2,140 coverages). The high-severity joint spall that caused the repair failure became more severe; however, no other joint

spalls increased in severity. Additional linear cracks developed. No interior corner breaks were observed on Repair 6 indicating that the combination of the slab thickness and foundation strength/thickness were adequate to support the heavy aircraft load. The parent slabs adjacent to the western trafficked edge had to be replaced before Repair 7 could take place.

Figure 50. Repair 6 progression of distresses.

(a) Shrinkage cracks at 0 passes

(b) Paste at joint starting to break up at 112 passes

(c) Spalling at joint on Quadrant #1 at 224 passes

(d) Spalling on Quadrant #2 at 768 passes

(e) Crack from Quadrant #1 to #3 at 768 passes

(f) Low-severity shattered slab in Quadrant #1 at 1,664 passes

Figure 51. Surface paste observed up to 112 passes.

Figure 52. Overview of Repair 6 at 2,112 passes.

4.1.7 Repair 7

Repair 7 was conducted after the replaced parent slabs had cured for at least 28 days. Repair 7 consisted of 10 in. of Rapid Set Concrete Mix® over 13.5 in. of cement-stabilized silty sand. The repair failed at approximately 896 passes (766 coverages) with high-severity joint spalling exceeding the failure criteria in two locations. The progression of distresses with increasing traffic can be found in Figure 53.

Figure 53. Repair 7 progression of distresses.

(a) No visible cracking on repair (Quadrant #3) at 0 passes

(b) Cracking in the paste at 112 passes

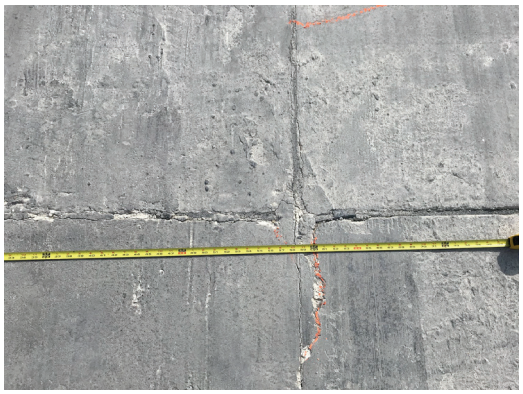

(c) Small corner break in center of repair at 112 passes

(d) Spalling in Quadrant #3 at 448 passes

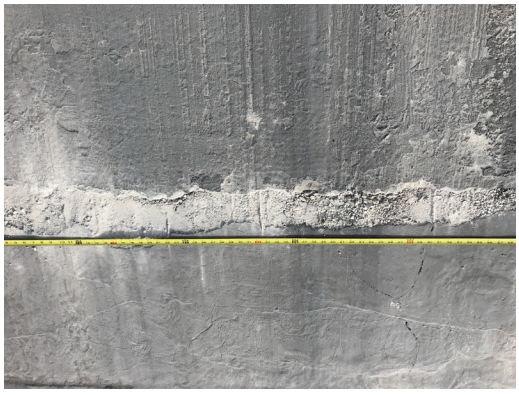

(e) Spalling in Quadrant #3 at 784 passes

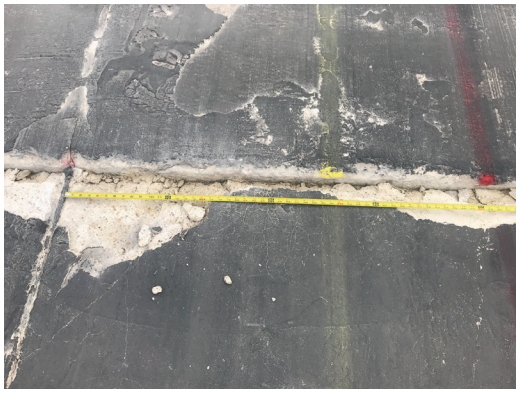

(f) Spalling in Quadrant #3 at 896 passes

The Rapid Set Concrete Mix® surface of Repair 7 had a higher slump than desired, causing an approximate 1-in.-thick paste to form on the surface of all quadrants. Nevertheless, no pavement distresses were noted on the repair before trafficking. After 112 passes (96 coverages), no spalling had developed; however, two quadrants developed interior corner breaks, and all four quadrants developed linear cracking. Joint spalling on the trafficked edges was observed after 336 passes (287 coverages). All four quadrants had low-severity shattered slabs (Figure 54), and the joint spalls became more severe after 448 passes (383 coverages). No additional cracking was observed after 784 passes (670 coverages); however, the joint spalls did progress in size. After 896 passes (766 coverages), a few additional low-severity linear cracks developed, and two joints spalls exceeded the failure criteria defined for this study (Figure 55).

Figure 54. Low-severity shattered slab at 448 passes.

Figure 55. Overview of repair 7 after 896 passes.

4.2 Post-traffic DCP results

DCP tests were conducted following the failure of each repair or after the completion of 3,500 passes (2,991 coverages). Results of post-traffic DCP tests are presented in Table 6. Post-traffic DCP tests revealed that the base and subgrade material for most pavement layers increased in strength during and after trafficking. The DCP measurement for Repair 6 showed the subgrade strength to have an average CBR of approximately 85%. This is an increase in strength of 60 CBR, which is not a typical strength for a clay material. It is assumed that rock from the base material was pushed through the subgrade material during the DCP tests.

Table 6. CBR post traffic values as measured using the DCP.

Repair No.	Base			Subgrade
	Thickness (in.)	Material	Average CBR (%)	Average CBR (%)
1	13.5	Flowable Fill	100	—[a]
2	14.0	Crushed Limestone	85	40
3	13.5	Flowable Fill	100	—[a]
4	20.0	Crushed Limestone	50	30
5	20.0	Crushed Limestone	100	30
6	16.0	Crushed Limestone	100	85[b]
7	13.5	Cement-Stabilized Silty Sand	100	—[a]

[a] Unable to measure due to refusal (CBR = 100) of base layer.

[b] Likely measured on top of rock that pushed through the subgrade layer.

4.3 Permanent deformation

During trafficking, the repairs were monitored for elevation changes by using a surveying rod and level in both the longitudinal (in the direction of traffic) and transverse directions (perpendicular to traffic), as shown previously in Figure 7 and Figure 8. The maximum change in elevation was recorded for most cases along the edges of the repairs in the locations of spalls. The maximum change in elevation measured in the location of the spalls is less than that measured during the inspection process with a ruler due to the inability to place the rectangular rod in the deepest portions of the spalled areas, as recorded in the previous section. These data show that no significant settlement or faulting occurred with these repairs and that the maximum change in elevation was less than 0.5 in.

4.4 HWD results

HWD tests were performed to evaluate the stiffness of the pavement structure of each repair and provide a baseline for subsequent comparison after traffic. The HWD data gave the impulse stiffness modulus (ISM) of the pavement structure as an indicator of the structural capacity of the pavement repairs. The ISM is the ratio of the applied load to the measured plate deflection where higher values represent a stiffer pavement structure.

Tests were performed at the center of each quadrant at 0 passes, 112 passes (96 coverages), and failure or 3,500 passes (2,991 coverages). Additional tests were conducted sporadically during trafficking for Repair 1 since failure was not immediately imminent. For all repairs, the HWD tests run at 0 passes occurred immediately before the start of traffic and approximately 2 hr after the last repair quadrant was placed.

The ISM values of each pavement structure with respect to C-17 load cart passes are plotted in Figure 56 and Figure 57. The plots show the stiffness of the pavement repairs relative to one another. The general trend for most of the repairs is a decrease in stiffness with an increase in passes and surface deterioration. However, Repairs 3, 6, and 7 showed an initial small spike of approximately 200 kips/in. at 112 passes (96 coverages). These three repairs each had a different backfill material and surface thickness when compared to each other.

Figure 56. ISM values with respect to C-17 load cart passes for Repairs 1 and 6.

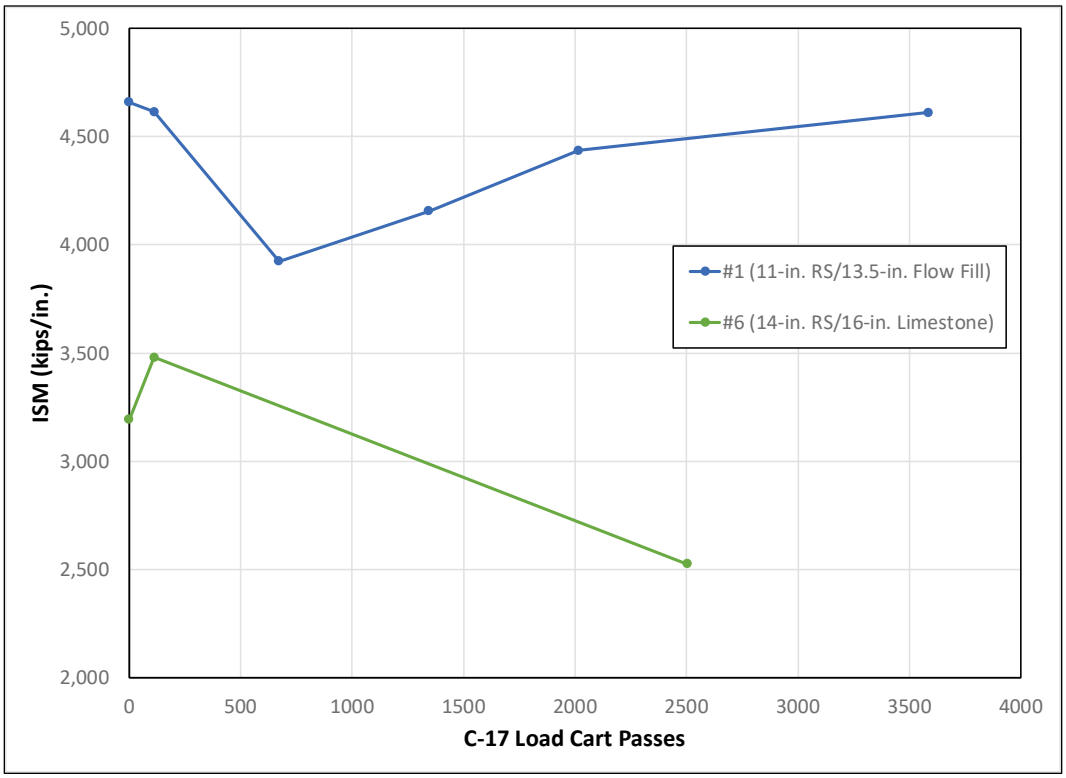

Figure 57. ISM values with respect to C-17 load cart passes for Repairs 2, 3, 4, 5, and 7.

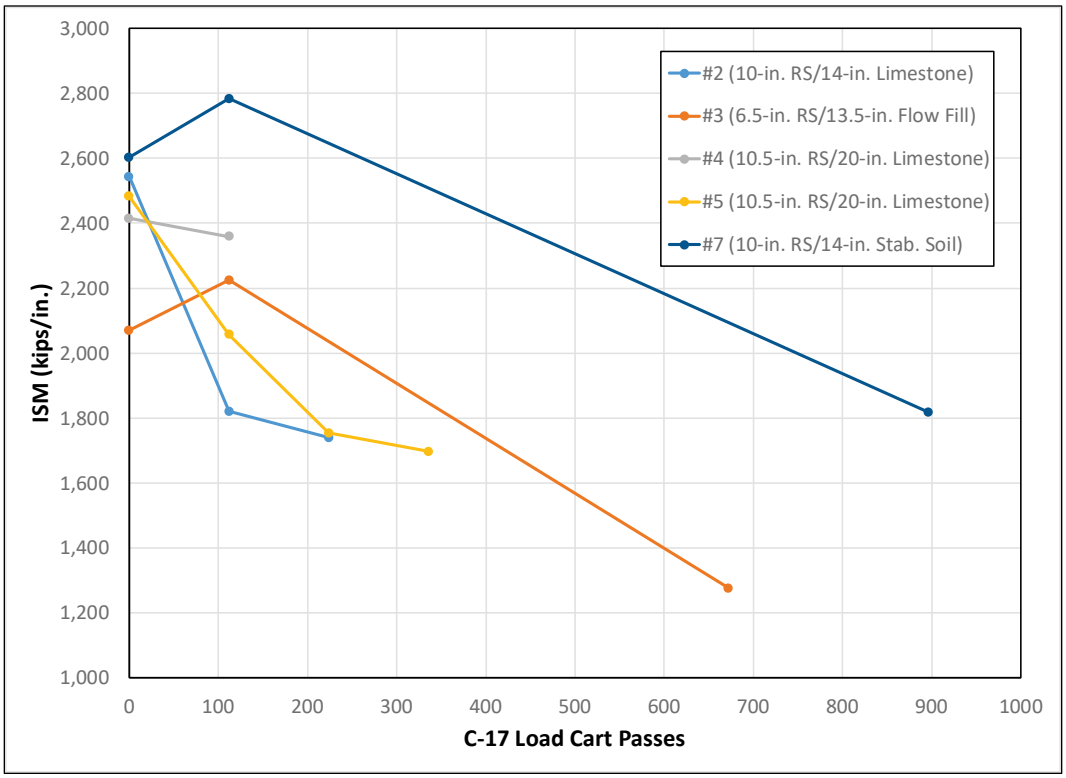

Repair 1 and Repair 6 shown in Figure 56 were the stiffest repairs. Repair 1 was stiff due to its 13.5-in.-thick rapid-setting flowable fill base material. Since flowable fill is a cementitious material, the repair behaved as though it had more than just an 11-in.-thick concrete surface cap. Repair 6 had 14 in. of a rapid-setting concrete surface and a 16-in.-thick crushed limestone base (100 CBR); however, the pavement structure of Repair 1 was still approximately 1,500 kips/in. stiffer at 0 passes. The difference in pavement stiffness increased between Repairs 1 and 6 as passes increased.

Repair 7, consisting of a 10-in.-thick rapid-setting concrete surface and 14 in. of stabilized soil, was the third stiffest pavement structure (Figure 57). Repair 7 had the same trend as Repair 6, which consisted of a small initial spike in ISM at 112 passes (96 coverages), then a decrease in stiffness with an increase in traffic. The small spike in stiffness is likely due to the continued hydration and curing of the stabilized soil early in the repair's service life.

Repair 3 had the thinnest concrete surface at 6.5 in. and also was the weakest pavement structure in terms of ISM. Repairs 2, 4, and 5 had similar pavement structures and similar stiffness values as measured by

using the HWD. Figure 57 shows that although Repairs 4 and 5 had six more inches of a crushed limestone base, the stiffness of the pavement structure was still similar to that of Repair 2. Repair 4 had a weaker base of approximately 50 CBR, while Repair 5's crushed limestone base was 100 CBR. The different base strengths had little observable effect on the HWD data. The stiffness of the repairs was most significantly affected by the concrete cap thickness and the use of the rapid-setting flowable fill as a backfill. As noted, the very high-strength and cementitious nature of the rapid-setting flowable fill provided significantly increased stiffness to the pavement structure.

4.5 Concrete properties

The Rapid-Set Concrete Mix® surfaces of each repair were tested for their 28-day compressive strengths in the laboratory at the Materials Testing Center at ERDC after core samples were extracted from the center of each repair quadrant (Table 7). The density of the cementitious materials was also measured for four of the seven repairs. The average 28-day compressive strengths for all 28 tests (four tests per repair) ranged from 6,200 to 10,200 psi and averaged 8,300 psi. The rapid-setting concrete exceeded the 5,000-psi compressive strength requirement for high-quality airfield PCC. The average density of the Rapid-Set Concrete Mix® was 141 lb/ft^3, ranging from 138 to 145 lb/ft^3.

Table 7. Rapid Set Concrete Mix® laboratory data of repairs.

Repair No.	Avg. 28-Day Compressive Strength (psi)	Average Density (lb/ft^3)
1	9,200	——[a]
2	8,700	——[a]
3	9,500	142
4	8,800	——[a]
5	7,400	139
6	7,300	141
7	7,300	142

[a] Not measured.

4.6 Summary

The typical surface distresses observed for the majority of the repairs, regardless of the base material or surface thickness, included shrinkage cracks, joint spalls, corner breaks, and low-severity shattered slabs.

Shrinkage cracks, considered a minor distress, were noted prior to traffic for many of the repairs. Shrinkage cracks are hairline cracks that are usually only a few feet long and do not extend across the entire slab or through the depth of the slab. They are formed during the curing of the concrete. Often, shrinkage cracks will appear if the rapid-setting concrete is placed too wet, generating a surface layer of paste, or is overworked by hand. While surface degradation of the excess paste layer under traffic generated FOD, the shrinkage cracking did not appear to contribute to the actual failure modes of the repairs (i.e., no tire hazard).

With the exception of Repair 6, which had the largest cap thickness, all large crater repairs had corner breaks in each quadrant's interior corner, or the center of the repair. Corner breaks are caused by load repetition combined with loss of foundation support and curling stresses. The parent slabs along the trafficking joints produced spalls. The center joints between the slabs typically did not spall. Spalling occurred at only the joints adjacent to the parent slabs in the trafficking area.

It was observed that increasing the base thickness of the crushed limestone backfill did not significantly improve the performance of the repair or change the failure mode. Two levels of passes, high and low, were achieved with the repairs that had crushed limestone or flowable fill as the base course material. A 6.5-in.-thick rapid-setting concrete surface with 13.5 in. of flowable fill backfill resulted in a failed repair at approximately 450 C-17 aircraft passes (385 coverages). Adding approximately 4.5 in. to the surface material with the same rapid-setting flowable fill backfill resulted in the ability to achieve 3,000 more passes (2,564 coverages) with the C-17 load cart.

A pass prediction chart for large crater repairs with C-17 aircraft traffic was created based on the results of this project. Figure 58 shows the prediction curves. The models were created using repairs backfilled with 13.5 in. of flowable fill or repairs backfilled with 20 in. of crushed stone. More data points with rapid-setting flowable fill or crushed limestone base course materials and Rapid-Set Concrete Mix® used for the repair surface are needed to prove the model. Previous testing of large crater repairs is listed in Table A2. However, the results are not included in Figure 58 because the quantitative failure criteria utilized in the testing described in this report were not yet implemented.

Figure 58. Prediction model for large crater repairs with a Rapid-Set Concrete Mix® surface and C-17 aircraft traffic.

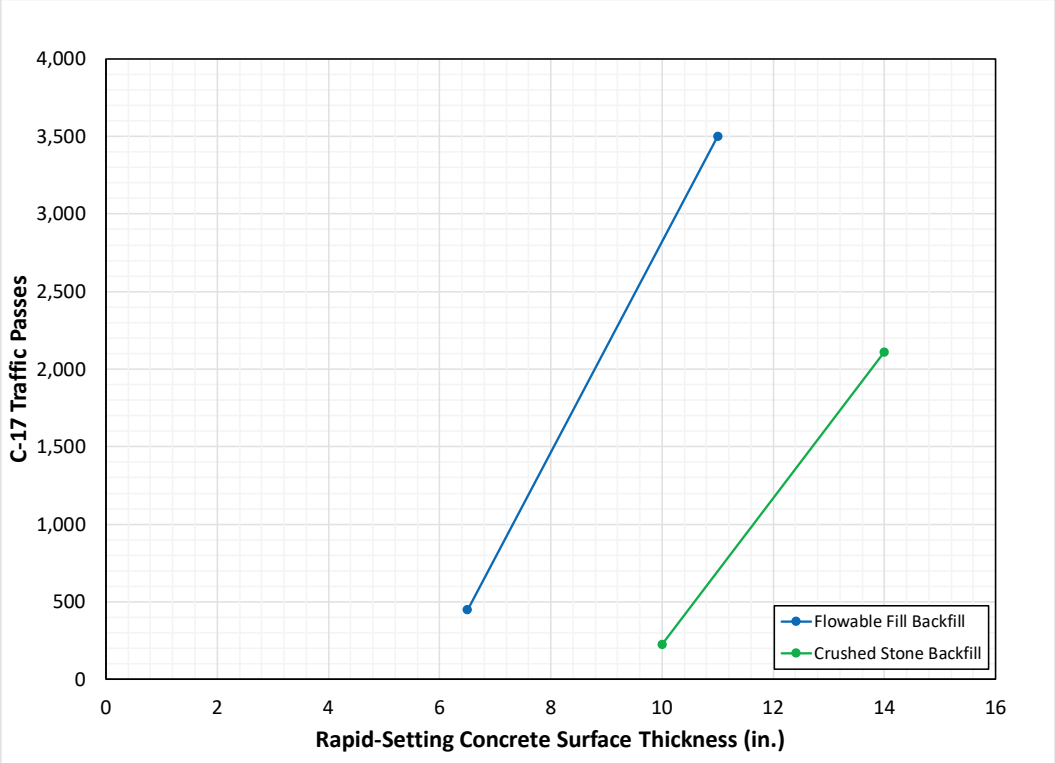

5 Conclusions and Recommendations

Seven large crater repairs using Rapid Set Concrete Mix® as the surface material and varying backfill materials and strengths were subjected to accelerated aircraft traffic using a multiple-wheel C-17 load cart. The base course or backfill materials varied from a medium-strength to high-strength crushed limestone, high-strength rapid-setting flowable fill, and high-strength cement-stabilized silty sand. The following conclusions and recommendations are given based on the results and observations from the large crater repair tests.

5.1 Conclusions

- The mode of failure for the large crater repairs, regardless of the surface thickness or backfill material, was primarily functional failure rather than structural failure due to high-severity joint spalling along the aircraft-trafficked repair joints.
- No settlement or faulting of the large crater repairs occurred.
- Shrinkage cracking appeared on the surface of almost all repairs. This was likely due to the fast curing and overworking of the rapid-setting concrete material.
- Minimal spalling occurred on the inside joints of the large crater repairs. Low-severity shattered slabs and interior corner breaks typically occurred on the surface, but the distresses did not result in the repairs' failure. The corner breaks do indicate inadequate foundation support for the applied load conditions.
- Rapid-setting concrete is capable of supporting at least 100 passes of aircraft passes for 30-ft repairs with a minimal surface thickness of 6 in.
- Rapid Set Concrete Mix® surface thickness influences the pavement structure and performance more than base thickness and strength.
- Rapid-setting flowable fill was challenging to place in large areas of 25 ft by 30 ft and 30 ft by 30 ft due to the nature of the water flowing to the shallow end of the repair area.
- Plastic forms for the surface placement work well for separating a large crater into quadrants.
- The Opperman Method of foam board placement, which includes attaching foam board to the plastic forms by using duct tape and screws, worked well and was the most efficient method for expansion board placement between repair quadrants.

- Placements of 10 to 14 in. of rapid-setting concrete surfaces per 15-ft by 15-ft quadrant does not push the limits of the volumetric mixer. It is recommended to wash the volumetric mixer after each quadrant to ensure the concrete residue in the mixer does not harden.

5.2 Recommendations

More data are needed to validate the large crater repair performance prediction curves created with this project by using the trafficking results of the repairs with flowable fill and crushed limestone backfill. Additional large crater repairs with different surface thicknesses of Rapid Set Concrete Mix® are needed to add clarity and extend the performance curve. Furthermore, additional repairs with cement-stabilized silty sand as the base course material are needed so that prediction curves can be produced. Additional data will provide the military with the ability to predict performance when repairing large craters with Rapid Set Concrete Mix® and a variety of backfill materials.

References

ASTM International. 2012. *Standard test methods for laboratory compaction characteristics of soil using modified effort (56,000 ft-lbf/ft³ (2,700 kN-m/m³))*. Designation: D1557-12e1. West Conshohocken, PA: American Society for Testing and Materials.

_____. 2014. *Standard test methods for specific gravity of soil solids by water pycnometer*. Designation: D854-14. West Conshohocken, PA: American Society for Testing and Materials.

_____. 2017a. *Standard practice for classification of soils for engineering purposes (Unified Soil Classification System)*. Designation: D2487-17e1. West Conshohocken, PA: American Society for Testing and Materials.

_____. 2017b. *Standard test methods for liquid limit, plastic limit, and plasticity index of soils*. Designation: D4318-17e1. West Conshohocken, PA: American Society for Testing and Materials.

_____. 2017c. *Standard test methods for particle-size distribution (gradation) of soils using sieve analysis*. Designation: D6913/D6913M-17. West Conshohocken, PA: American Society for Testing and Materials.

_____. 2017d. *Standard test methods for in-place density and water content of soil and soil-aggregate by nuclear methods (shallow depths)*. Designation: D6938-17a. West Conshohocken, PA: American Society for Testing and Materials.

_____. 2018a. *Standard test method for flexural strength of concrete (using simple beam with third-point loading)*. Designation: C78/C78M-18. West Conshohocken, PA: American Society for Testing and Materials.

_____. 2018b. *Standard test method for airport pavement condition index surveys*. Designation: D5340-12. West Conshohocken, PA: American Society for Testing and Materials.

_____. 2018c. *Standard test method for use of the dynamic cone penetrometer in shallow pavement applications*. Designation: D6951/D6951M-18. West Conshohocken, PA: American Society for Testing and Materials.

_____. 2020. *Standard test method for compressive strength of cylindrical concrete specimens*. Designation: C39/C39M-20. West Conshohocken, PA: American Society for Testing and Materials.

Barna, L. A., J. S. Tingle, and P. S. McCaffrey. 2010. *Laboratory and field evaluation of rapid setting cementitious materials for large crater repair*. ERDC/CRREL TR-10-4. Hanover, NH: U.S. Army Engineer Research and Development Center.

Bell, H. P., L. Edwards, W. D. Carruth, J. S. Tingle, and J. R. Griffin. 2013. *Wet weather crater repair testing at Silver Flag Exercise Site, Tyndall Air Force Base, Florida*. ERDC/GSL TR-13-42. Vicksburg, MS: U.S. Army Engineer Research and Development Center.

Carruth, W. D., L. Edwards, H. P. Bell, J. S. Tingle, J. R. Griffin, and C. A. Rutland. 2015. *Large crater repair at Silver Flag Exercise Site, Tyndall Air Force Base, Florida*. ERDC/GSL TR-15-27. Vicksburg, MS: U.S. Army Engineer Research and Development Center.

Edwards, L., H. P. Bell, W. D. Carruth, J. R. Griffin, and J. S. Tingle. 2013. *Cold weather crater repair testing at Malmstrom Air Force Base, Montana*. ERDC/GSL TR-13-32. Vicksburg, MS: U.S. Army Engineer Research and Development Center.

Priddy, L. P. 2011. *Development of laboratory testing criteria for evaluating cementitious, rapid-setting pavement repair materials*. ERDC/GSL TR-11-13. Vicksburg, MS: U.S. Army Engineer Research and Development Center.

Priddy, L. P., H. P. Bell, L. Edwards, W. D. Carruth, and J. F. Rowland. 2016 *Evaluation of the structural performance of CTS Rapid Set Concrete Mix®*. ERDC/GSL TR-20-16. Vicksburg, MS: U.S. Army Engineer Research and Development Center.

Priddy, L. P., J. R. Griffin, and J. S. Tingle. 2011. *Live-flight certification testing of critical runway assessment and repair (CRATR) technologies, Avon Park Air Force Range, Florida*. ERDC/GSL TR-11-7. Vicksburg, MS: U.S. Army Engineer Research and Development Center.

Priddy, L. P., J. S. Tingle, M. C. Edwards, J. R. Griffin, and T. J. McCaffrey. 2013. *CRATR technology demonstration: Limited operational utility assessment 2*. ERDC/GSL TR-13-39. Vicksburg, MS: U.S. Army Engineer Research and Development Center.

Robinson, J. H., and C. P. Rabalais. 1993. *Performance of the combat engineer vehicle with mineplow operating worldwide and in theaters of operations*. Technical Report GL-93-23. Vicksburg, MS: U.S. Army Engineer Waterways Experiment Station.

Unified Facilities Criteria (UFC). 2001. *Pavement design for airfields*. UFC 03-260-02. Construction Criteria Base. Washington, DC: National Institute of Building Sciences.

Webster, S. L., R. W. Brown, and J. R. Porter. 1994. *Force projection site evaluation using the electric cone penetrometer (ECP) and the dynamic cone penetrometer (DCP)*. Technical Report GL-94-17. Vicksburg, MS: U.S. Army Waterways Experiment Station.

Appendix A: Additional Data and Repair Notes

Figure A1. Particle-size distribution report for limestone.

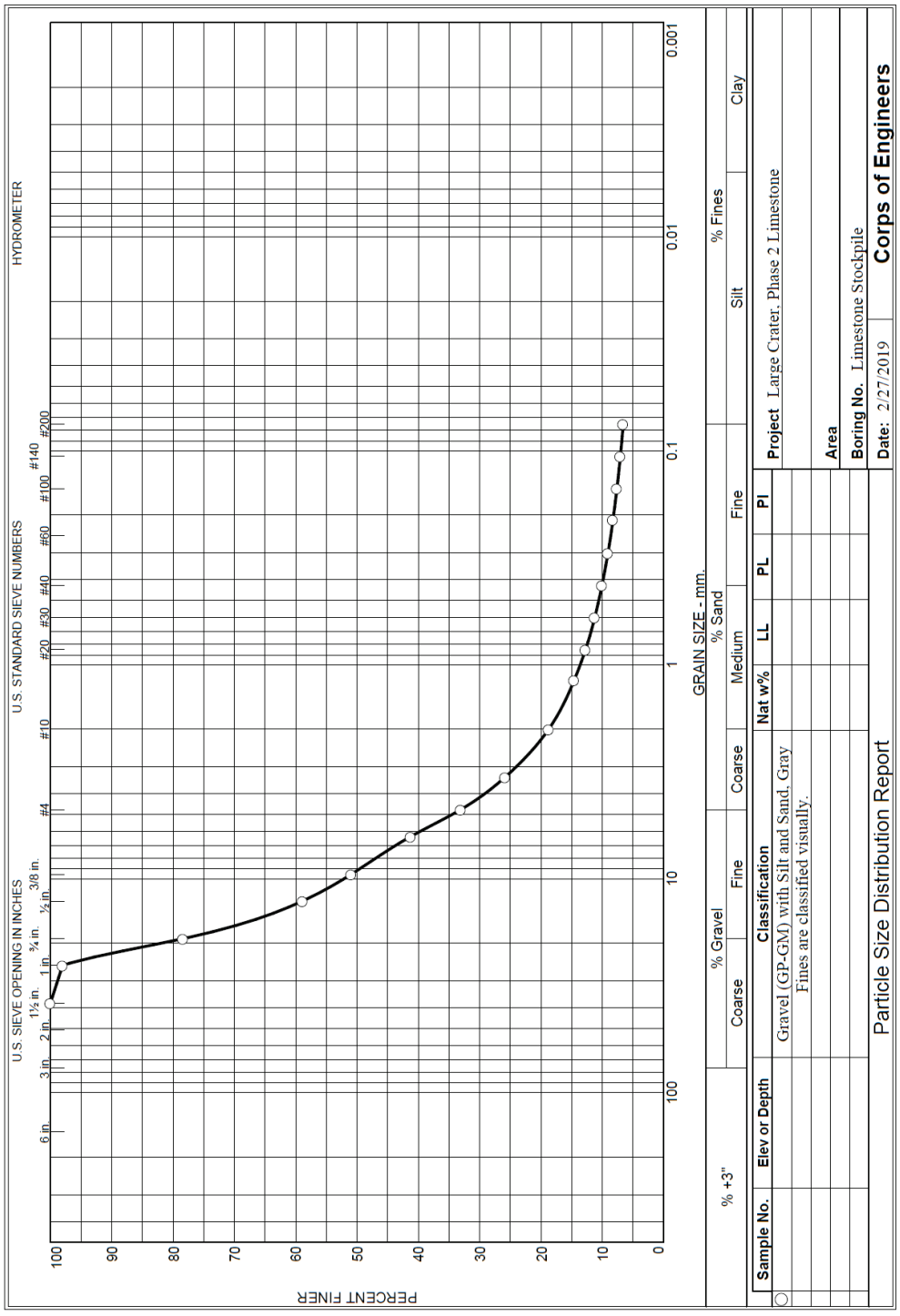

Figure A2. Particle-size distribution report silty sand.

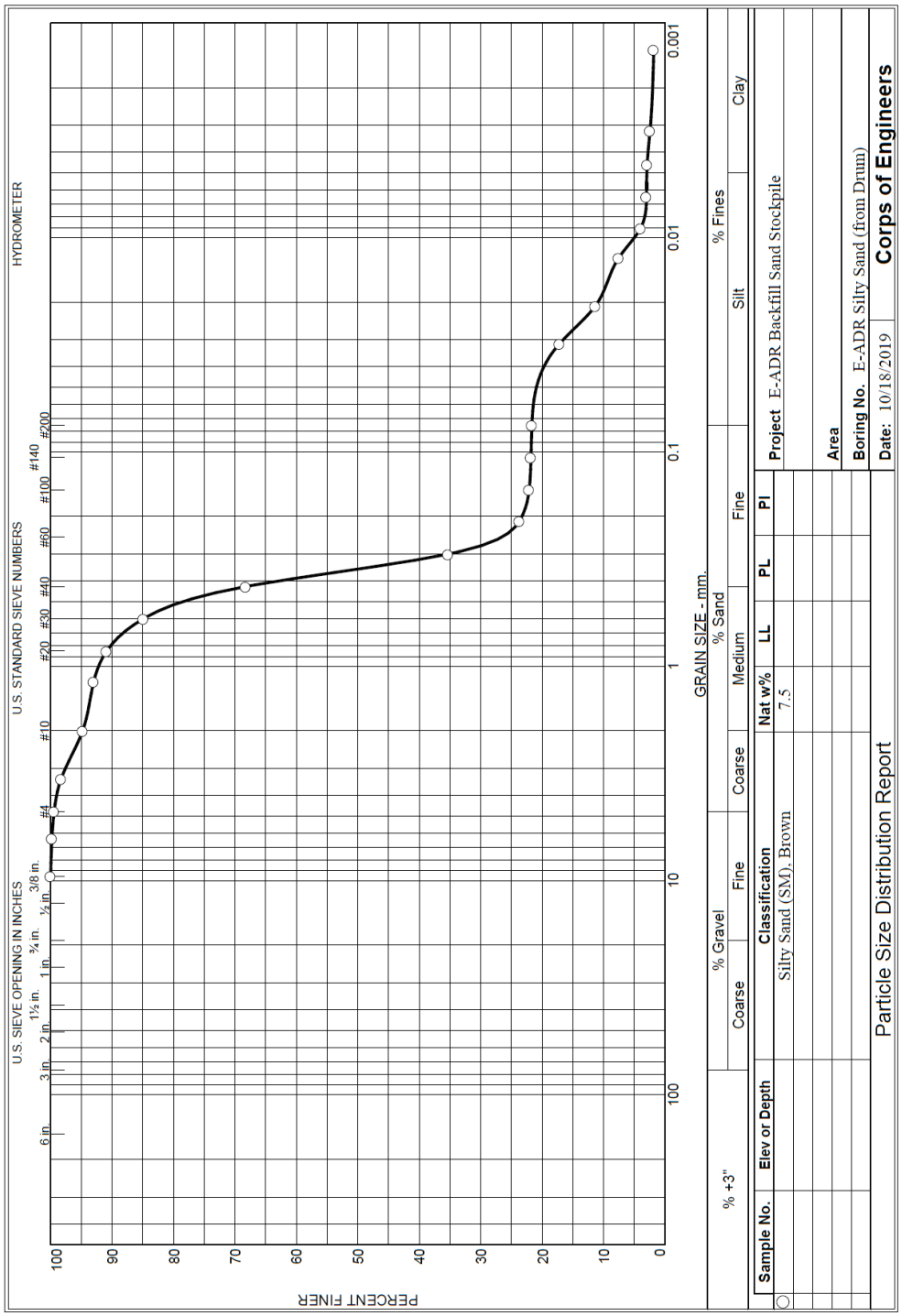

Figure A3. Particle-size distribution report for the CL soil used for the subgrade material in Repairs 1 through 4.

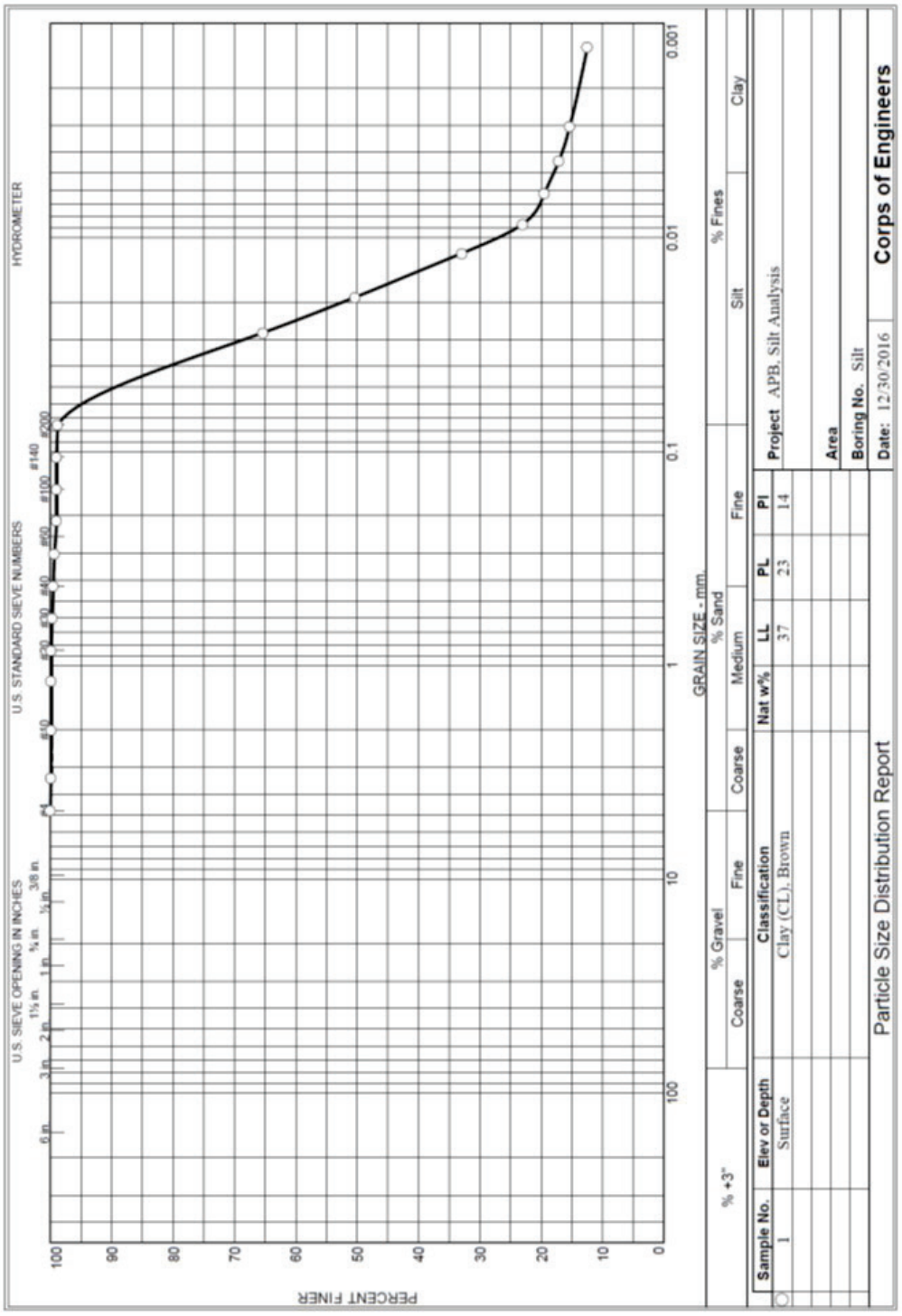

Figure A4. Particle-size distribution report for the CL soil used for the subgrade material in Repairs 5 through 7.

Table A1. Large crater repair distresses during trafficking.

Repair	Description	Passes	Visual Observation	FOD Potential
1	11-in. cap/ 13.5 in. flow fill	0	No distresses were noted.	None
		112	Low-severity corner breaks began around 56 passes. By 112 passes, corner breaks developed in the center of the repair (one in each repair quadrant).	None
		250	Low-severity joint spalling began occurring on the western and eastern trafficked edges. The biggest joint spall was along the eastern edge in Quadrant #4 and was 16 in. long, 3.5 in. wide, and 1.3 in. deep. Minimal FOD of 0.5 in. along the western joint was observed.	Low
		336	No changes were observed.	Low
		448	The interior corner breaks on Quadrants #3 and #4 began spalling with 1.25-in.-sized FOD. New low-severity joint spalls developed along the eastern and western trafficked edges.	Low
		672	The spalls along the corner breaks of Quadrants #2 and #4 opened up and were 1.25 in. wide and 1.75 in. deep, respectively. The largest joint spall was along the eastern trafficked edge and was 28 in. long, 1.75 in. wide, and 1.25 in. deep. Maximum-sized FOD of 1.5 in. was observed around the eastern joint spall.	Low
		1,008	No changed were observed to the center corner breaks. The western joint spall was 31 in. long, 1.75 in. wide, and 1.5 in. deep. The eastern joint spall was 59 in. long, 2 in. wide, and 1.75 in. deep. Minimal FOD with a maximum size of 1 in. was observed along both trafficked edges.	Low
		1,344	No changed were observed to the center corner breaks. The largest joint spall along the eastern trafficked edge was 63 in. long, 3 in. wide, and 2.5 in. deep. The western joint spall was 42 in. long, 1.75 in. wide, and 1.75 in. deep. Minimal FOD was observed.	Low
		1,680	Large 2-in. FOD was observed coming from the interior corner breaks. The deepest and widest spall coming from one of the interior corner breaks was 2.75 in. wide and 2 in. deep. The joint spalls along the trafficked edge did not change much. The parent slabs adjacent to the trafficking edges began spalling.	Low
		2,016	The FOD was not noted because the repair was cleared of debris before collecting data. The interior corner breaks had spalls that were no larger than 2.75 in. wide and 2.25 in. deep. The largest spall along the western trafficked edge was 42 in. long, 1.75 in. wide, and 1.75 in. deep. The largest spall along the eastern trafficked edge was 63 in. long, 3 in. wide, and 2.5 in. deep.	Low
		2,576	The FOD was not noted because the repair was cleared of debris before collecting data. The interior corner breaks had not changed in size. The largest spall along the western trafficked edge was 43 in. long, 1.75 in. wide, and 1.75 in. deep. The largest spall along the eastern trafficked edge was 63 in. long, 3.25 in. wide, and 3 in. deep.	Low
		3,024	The FOD was cleaned before the repair was formally documented. The largest spall from the interior corner breaks was 3.25 in. wide and 2.25 in. deep. The largest spall along the western trafficked edge was 42 in. long, 1.75 in. wide, and 1.75 in. deep. The largest spall along the eastern trafficked edge was 63 in. long, 3.25 in. wide, and 3.25 in. deep.	Low
		3,584	The repair failed due to a tire hazard from high-severity spalling along the center interior cracks. The largest spall along the center interior cracks was 3.25 in. wide, and 2.75 in. deep. The maximum-sized joint spalling along the eastern trafficked edge was 63 in. long, 3.5 in. wide, and 3.25 in. deep. The maximum-sized joint spalling along the western trafficked edge was 43 in. long, 1.75 in. wide, and 1.75 in. deep.	Low

Repair	Description	Passes	Visual Observation	FOD Potential
2	10-in. cap/14 in. crushed limestone	0	Repair has a few shrinkage cracks on the surface of each repair quadrant.	None
		18	Corner break developed in Quadrant #4.	None
		20	Corner break developed in Quadrant #2.	None
		22	Corner break developed in Quadrant # 1.	None
		26	Corner break developed in Quadrant #3.	None
		112	All repair quadrants developed joint spalling along the trafficking edges. Quadrants # 1, 3, and 4 were low-severity shattered slabs. Repair Quadrant #2 developed an additional corner break in the interior corner along the western trafficked edge. The interior corner breaks were not spalling. All trafficked edges developed spalling. The maximum-sized joint spalling along the eastern trafficked edge was 58 in. long, 7 in. wide, and 1.875 in. deep. The maximum-sized joint spalling along the western trafficked edge was 74 in. long, 6 in. wide, and 2.875 in. deep.	High
		224	The repair was failed due to the spalling along the western trafficked edge. The maximum-sized joint spalling along the western trafficked edge was 74 in. long, 6 in. wide, and 3 in. deep. The maximum-sized joint spalling along the eastern trafficked edge was 58 in. long, 7.25 in. wide, and 1.875 in. deep.	High
3	6.5-in. cap/13.5 in. flow fill	0	Very few shrinkage cracks were observed in Quadrants # 2, 3, and 4. Quadrant #1 had a 1-in. spall on the western joint.	None
		112	The joint spall on the western joint of Quadrant # 1 was 12 in. long, 1.25 in. wide, and 0 in. deep. A corner break in the repair's interior of Quadrant # 1 was developing but had not reached the south joint.	None
		336	Joint spalling on the parent slabs of all the trafficked edges with 1- to 2-in. FOD was noted. Smaller sized FOD from 0.375 to 0.75 in. was observed on the repair. Quadrants # 1, 3, and 4 were shattered, and all quadrants had spalls along the trafficked edges. Quadrant # 2 did not have any cracks. The largest spall along the western trafficked edge was 66 in. long, 5 in. wide, and 0.125 in. deep, and the largest spall along the eastern trafficked edge was 90 in. long, 11 in. wide, and 0.75 in. deep.	Moderate
		392	No new cracks were observed. The joint spalls along the trafficked edges increased in size and severity. Some of the FOD ranged from 2 to 12 in. in size. The largest spall along the western trafficked edge was 66 in. long, 6 in. wide, and 0.625 in. deep, and the largest spall along the eastern trafficked edge was 91 in. long, 11 in. wide, and 1.25 in. deep.	High
		448	The FOD was not measured because the repair was cleaned before data was collected. However, larger FOD was observed on the east edge, and slightly smaller FOD was observed on the west edge. The largest spall along the western trafficked edge was 66 in. long, 6.5 in. wide, and 1.25 in. deep, and the largest spall along the eastern trafficked edge was 106 in. long, 11 in. wide, and 2 in. deep. The repair was considered failed due to the size of the joint spall along the eastern trafficked edge and the size of the FOD.	High
		504	The repair looked about the same. Quadrant # 2 was broken up slightly more, however.	Low
		560	Minimal changes were observed. Minimal FOD was noted on the western edge. The largest spall along the western trafficked edge was 67 in. long, 6.5 in. wide, and 1.375 in. deep, and the largest spall along the eastern trafficked edge was 106 in. long, 11 in. wide, and 2 in. deep.	Low
		616	No changes were observed. Minimal FOD was noted on the western edge.	Low

Repair	Description	Passes	Visual Observation	FOD Potential
		672	New cracks were observed in Quadrants # 1 and # 2. The parent slabs were spalling with large FOD. FOD ranging from 0.125 to 1 in. in size was noted around spalls along the trafficked edges. The largest spall along the western trafficked edge was 84 in. long, 7 in. wide, and 1.625 in. deep, and the largest spall along the eastern trafficked edge was 137 in. long, 15 in. wide, and 2.25 in. deep.	
4	10.5-in. cap/ 20 in. crushed limestone	0	Repair Quadrant # 1 had very few shrinkage cracks. A crack was developing from the northern joint of repair Quadrant # 2, but it had not reached the southern joint yet.	None
		112	The shrinkage cracks on Quadrant #1 opened up some. Interior corner breaks developed in all repair quadrants. The crack from Quadrant # 2 extended to reach the south joint, and two new cracks formed; Quadrant # 2 is shattered. Quadrant # 3 developed another corner break in its northwestern interior location. No joint spalls were present.	Low
		224	The repair was failed due to joint spalling along the western edge. All repair quadrants are shattered. Joint spalling developed along the trafficked joints. The largest joint spall along the western edge was 104 in. long, 6 in. wide, and 2.125 in. deep. The largest spall along the eastern edge was 57 in. long, 8 in. wide, and 1.5 in. deep.	Moderate
		336	The cracks appeared to be slightly larger and more spalled. The joint spalls increased in size. The repair had moderate FOD with of 1.5 in. The largest joint spall along the western edge was 117 in. long, 7.75 in. wide, and 2.25 in. deep. The largest spall along the eastern edge was 83 in. long, 9 in. wide, and 2.375 in. deep.	Moderate
		500	All four repair quadrants were shattered slabs. The largest joint spall along the western edge was 148 in. long, 8.5 in. wide, and 2.875 in. deep. The largest spall along the eastern edge was 105 in. long, 8 in. wide, and 2.75 in. deep.	Moderate
5	10.5-in. cap/ 20 in. crushed limestone	0	The edges of the repair had overflow of the rapid-setting concrete cap when it was placed too wet. Shrinkage cracking was noted on all repair quadrants.	None
		112	Two low-severity linear cracks extended from the west joint to the east joint of Quadrant # 1. A low-severity crack extended from the north joint to the south joint of Quadrant # 2. No joint spalling was observed.	None
		224	Repair Quadrants # 1, 2, and 3 were shattered slabs. Quadrant # 4 had shrinkage cracking. Joint spalling was observed on both trafficking edges; however, more spalling was noted on the west edge. The maximum FOD sizes were 1 to 4 in. The largest spall on the western edge was 88 in. long, 9 in. wide, and 2 in. deep. The largest spall on the eastern edge was 80 in. long, 5 in. wide, and 1.5 in. deep.	High
		274	No new cracks were observed on the repair. The repair was considered failed due to the size of the spall on the western trafficked edge. The largest spall on the western edge was 90 in. long, 12 in. wide, and 2.25 in. deep. The largest spall on the eastern edge was 92 in. long, 10 in. wide, and 1.5 in. deep. The maximum FOD size was 1 to 2 in.	High
		336	The parent slabs adjacent to Quadrants # 2 and # 4 are severely spalled. The largest spall on the western edge was 102 in. long, 12 in. wide, and 2.5 in. deep. The largest spall on the eastern edge was 94 in. long, 10 in. wide, and 2.125 in. deep.	High
6	14-in. cap/16 in. crushed limestone	0	A large amount of shrinkage cracks developed over the entire repair.	None
		112	No changes were observed.	None
		224	Joint spalling was observed along the trafficked edges. A large amount of 0.25- to 1-in.-sized FOD was noted along the western joint of Quadrant # 2. The largest spall on the western edge was 118 in. long, 5 in. wide, and 1 in. deep. The largest spall on the eastern edge was 39 in. long, 4 in. wide, and 1 in. deep.	Moderate

Repair	Description	Passes	Visual Observation	FOD Potential
		336	FOD ranging from 0.25 to 0.5 in. was noted around the joint spalling. The largest spall on the western edge was still 118 in. long, 5 in. wide, and 1 in. deep. The largest spall on the eastern edge was 77 in. long, 4 in. wide, and 1 in. deep.	Moderate
		448	Minimal FOD along the joint spalls was observed. The maximum FOD size was 0.5 in. The largest spall on the western edge was 144 in. long, 5 in. wide, and 1.375 in. deep. The largest spall on the eastern edge was still 77 in. long, 4 in. wide, and 1 in. deep.	Moderate
		768	No FOD was noted because the repair was swept before data was collected. New cracks developed in Quadrants # 1 and # 3; however, the cracks did not extend from joint to joint yet. The largest spall on the western edge was 144 in. long, 10 in. wide, and 1.875 in. deep. The largest spall on the eastern edge was 101 in. long, 7 in. wide, and 1.5 in. deep.	Moderate
		1,664	No FOD was noted because the repair was swept before data was collected. Quadrant # 1 was a low-severity shattered slab. Quadrant # 3 developed an additional low-severity crack. The largest spall on the western edge was 144 in. long, 10 in. wide, and 2 in. deep. The largest spall on the eastern edge was 101 in. long, 7 in. wide, and 1.5 in. deep.	Moderate
		2,112	The maximum-sized FOD was 1.5 in., which was noted on the west edge of Quadrant # 2. The east edge of Quadrant # 3 had a minimal amount of 0.25-in. FOD. Quadrant # 4 had a new crack extending from the west to east joints. The largest spall on the western edge was 144 in. long, 10 in. wide, and 2.25 in. deep. The largest spall on the eastern edge was 101 in. long, 7.5 in. wide, and 1.5 in. deep.	Moderate
		2,504	Additional cracking was noted on Quadrants # 1 and # 2. The maximum-sized FOD was 2.5 in., which was noted on the west edge of Quadrant # 2. The east edge of Quadrant # 3 had a minimal amount of 0.25-in. FOD. The largest spall on the western edge was 144 in. long, 10 in. wide, and 3.75 in. deep. The largest spall on the eastern edge was 77 in. long, 4 in. wide, and 1 in. deep. Parent slabs adjacent to the west end of the repair are failed with high-severity shattered slabs and were replaced before starting with Repair 7.	Moderate
7	10-in. cap/13.5 in. stabilized silty sand	0	No distresses were noted.	None
		112	Several cracks, including corner breaks, formed in Quadrants # 2 and # 3. Quadrants # 1 and # 4 had one crack each. No joint spalls and no FOD were noted.	None
		336	Minimal FOD was noted mainly near the center joints. Quadrant # 4 had a corner break at the interior of the repair. Joint spalls had developed on the trafficked edges. The largest joint spall on the western edge was 6 in. long, 1.5 in. wide, and 0.25 in. deep. The largest joint spall on the eastern edge was 55 in. long, 3.5 in. wide, and 0.375 in. deep.	Low
		448	Quadrant # 1 developed a corner break at the interior of the repair. All repair quadrants were low-severity shattered slabs. The FOD ranged from 0.25 in. to 0.75 in. in size. The largest joint spall on the western edge was 23 in. long, 3 in. wide, and 0.5 in. deep. The largest joint spall on the eastern edge was 90 in long, 3.5 in. wide, and 1.375 in. deep.	Moderate
		672	No new cracks were observed. The FOD was between 0.25 and 0.5 in. in size. The largest spall on the western edge was 24 in. long, 6 in. wide, and 0.625 in. deep. The largest spall on the western edge was 92 in. long, 5 in. wide, and 1.375 in. deep.	Moderate
		784	The FOD on the west edge was minimal and no more than 0.25 in. in size. The largest joint spall on the western edge was 24 in. long, 6.25 in. wide, and 0.125 in. deep. The FOD on the east edge ranged from 0.5 to 1 in. in size. The largest joint spall on the eastern edge was 93 in. long, 8.5 in. wide, and 1.375 in. deep.	Moderate
		896	Quadrants # 2, 3, and 4 had one new crack each. The existing cracks were getting wider, but they were still low severity. The repair failed due to the size of the joint spall and also a tire hazard on the eastern trafficked edge. The repair was swept before data was collected, so the FOD size was not noted. The largest spall on the western edge was 24 in. long, 7 in. wide, and 1.875 in. deep. The largest spall on the eastern edge was 106 in. long, 13 in. wide, and 2.5 in. deep.	Moderate

Table A2. Large crater repair summary from previous testing by ERDC.

Repair Size	SURFACE			BASE			Traffic Type	Passes to Failure	Technical Report
	Avg. Thickness (in.)	Material	28-Day Avg. Compressive Strength (psi)	Avg. Thickness (in.)	Material	CBR (%)			
32' X 30'	8.26	Stone and grout (control)		12 - 16	crushed concrete	30	F-15E	5,008[a]	TR-10-4
32' X 30'	9.05	CeraTech, Pavement EX-H™		12 - 16	crushed concrete	30	F-15E	5,008[a]	TR-10-4
30' X 30'	8.11	Ultimax™ Concrete		12 - 16	crushed concrete	>30	F-15E	5,008[a]	TR-10-4
30' X 30'	8.39	Degussa, ThoRoc™ 10-61		12 - 16	crushed concrete	25	F-15E	5,008[a]	TR-10-4
30' X 30'	8.68	CTS Rapid Set®, DOT mix		12 - 16	crushed concrete	25	F-15E	5,008[a]	TR-10-4
25' X 30'	11.00	CTS Rapid Set®, AC mix	9,200	13.5	Buzzi Unicem Utility Fill 1-Step 750	100	C-17	3,500[b]	current
25' X 30'	10.00	CTS Rapid Set®, AC mix	8,700	14.0	crushed limestone	65	C-17	100[b]	current
25' x 30'	6.50	CTS Rapid Set®, AC mix	9,500	13.5	Buzzi Unicem Utility Fill 1-Step 750	100	C-17	450[b]	current
25' x 30'	10.50	CTS Rapid Set®, AC mix	8,800	20	crushed limestone	50	C-17	225[b]	current
30' X 30'	10.50	CTS Rapid Set®, AC mix	7,400	20	crushed limestone	85	C-17	225[b]	current
30' X 30'	14.00	CTS Rapid Set®, AC mix	7,300	16	crushed limestone	100	C-17	1,600[b]	current
30' X 30'	10.00	CTS Rapid Set®, AC mix	7,300	13.5	cement-stabilized silty sand	75	C-17	900[b]	current
30' X 30'	12.44	CTS Rapid Set®, AC mix	7,770	11.6	crushed limestone	45	C-17	400[c]	TR-15-27
30' X 30'	10.19	CTS Rapid Set®, AC mix	8,208	12	Buzzi Unicem Utility Fill 1-Step 750	92	C-17	1,500[d]	TR-15-27
30' X 30'	10.38	CTS Rapid Set®, AC mix	8,253	10 to 12	Buzzi Unicem Utility Fill 1-Step 750	100	C-17	1,500[e]	TR-15-27

[a] Traffic stopped at 5,008 passes with typical large crater surface distresses; failure was not defined in the report.

[b] Failure was defined as a joint spall that is at least 2 ft long, 6 in. wide, and 2 in. deep; a high-severity shattered slabs; or a tire hazard.

[c] Traffic stopped at 400 passes due to medium-severity shattered slab, medium-severity corner spalling, and medium-severity corner breaks.

[d] Traffic stopped at 1,500 passes due to medium-severity joint spall and medium-severity linear cracking.

[e] Traffic stopped at 1,500 passes due to medium-severity interior corner breaks and high-severity joint spalling.

Unit Conversion Factors

Multiply	By	To Obtain
cubic feet	0.02831685	cubic meters
degrees Fahrenheit	(F-32)/1.8	degrees Celsius
feet	0.3048	meters
gallons (U.S. liquid)	3.785412 E-03	cubic meters
inches	0.0254	meters
pounds (mass)	0.45359237	kilograms
pounds (force) per cubic foot	16.0185	kilograms per cubic meter
pounds (force) per square inch	6.894757	kilopascals
square inches	6.4516 E-04	square meters

REPORT DOCUMENTATION PAGE

Form Approved
OMB No. 0704-0188

1. REPORT DATE *(DD-MM-YYYY)*	**2. REPORT TYPE**	**3. DATES COVERED** *(From - To)*
June 2021	Final	

4. TITLE AND SUBTITLE

Alternatives for Large Crater Repairs using Rapid Set Concrete Mix®

5a. CONTRACT NUMBER

5b. GRANT NUMBER

5c. PROGRAM ELEMENT NUMBER

6. AUTHOR(S)

Lulu Edwards, Haley P. Bell, and Marcus L. Opperman

5d. PROJECT NUMBER

5e. TASK NUMBER

5f. WORK UNIT NUMBER

7. PERFORMING ORGANIZATION NAME(S) AND ADDRESS(ES)

Geotechnical and Structures Laboratory
U.S. Army Engineer Research and Development Center
3909 Halls Ferry Road
Vicksburg, MS 39180-6199

8. PERFORMING ORGANIZATION REPORT NUMBER

ERDC/GSL TR-21-16

9. SPONSORING / MONITORING AGENCY NAME(S) AND ADDRESS(ES)

Headquarters, U.S. Air Force Civil Engineer Center
Tyndall Air Force Base, FL 32403-5319

10. SPONSOR/MONITOR'S ACRONYM(S)

11. SPONSOR/MONITOR'S REPORT NUMBER(S)

12. DISTRIBUTION / AVAILABILITY STATEMENT

Approved for public release; distribution is unlimited.

13. SUPPLEMENTARY NOTES

MIPR F4ATA78038GW01

14. ABSTRACT

Research was conducted at the U.S. Army Engineer Research and Development Center (ERDC) in Vicksburg, MS, to identify alternative repair methods and materials for large crater repairs using Rapid Set Concrete Mix®. This report presents the technical evaluation of the field performance of full-depth slab replacement methods conducted using Rapid Set Concrete Mix® over varying strength foundations. The performance of each large crater repair was determined by using a load cart representing one-half of the full gear of a C-17 aircraft. Results indicate that using rapid-setting concrete is a viable material for large crater repairs, and the performance is dependent on surface thickness and base strength.

15. SUBJECT TERMS

Airfield damage repair
Large crater
Cratering
Rapid-setting cement
Flowable fill
Cement-stabilized base
Concrete slabs
Military bases
Runways (Aeronautics)—Maintenance and repair
Concrete—Mixing
Concrete—Additives

16. SECURITY CLASSIFICATION OF:			**17. LIMITATION OF ABSTRACT**	**18. NUMBER OF PAGES**	**19a. NAME OF RESPONSIBLE PERSON**
a. REPORT	**b. ABSTRACT**	**c. THIS PAGE**			**19b. TELEPHONE NUMBER** *(include area code)*
Unclassified	Unclassified	Unclassified	SAR	87	